

8 **Self-excited Oscillations in the Atmosphere (0 – 110 km)**
9 **at Long Periods**

10 Dirk Offermann(1), Christoph Kalicinsky(1), Ralf Koppmann(1), and Johannes
11 Wintel(1,2)
12
13
14

- 15
16 (1) Institut für Atmosphären - und Umweltforschung, Bergische Universität Wuppertal,
17 Wuppertal, Germany
18 (2) Now at Elementar Analysensysteme GmbH, Langenselbold, Germany
19
20
21
22
23

24 Corresponding author: Dirk Offermann, (offer@uni-wuppertal.de)
25
26
27

- 28 Key Points: - multi-decadal oscillations in GCM and measurements
29 - self-excited oscillations **related** to the atmosphere basic dynamics
30 - vertical amplitude and phase structure similar for all oscillation periods
31
32
33
34
35
36
37
38
39
40
41
42
43
44
45
46
47
48
49

51
52
53
54
55
56
57
58
59
60
61
62
63
64
65
66
67
68
69
70
71
72
73
74
75
76
77
78
79
80
81
82
83
84
85
86
87
88
89
90
91
92
93
94
95
96
97
98
99
100
101

Self-generated oscillations have been observed in measured atmospheric data at multi-annual periods. These oscillations are also present in General Circulation Models even if their boundary conditions with respect to solar cycle, sea surface temperature, and trace gas variability are kept constant. The present analysis contains temperature oscillations with periods from below 5 yr up to above 200 yr in an altitude range from the Earth's surface to the lower thermosphere (110 km). The periods are quite robust as they are found to be the same in different model calculations and in atmospheric measurements. The oscillations show vertical profiles with special structures of amplitudes and phases. They form layers of high / low amplitudes that are a few dozen km wide. Within the layers the data are correlated. Adjacent layers are anticorrelated. A vertical displacement mechanism is indicated with displacement heights of a few 100 metres. Vertical profiles of amplitudes and phases of the various oscillation periods as well as their displacement heights are surprisingly similar. The oscillations are related to the thermal and dynamical structure of the middle atmosphere. These results are from latitudes/longitudes in Central Europe.

Short summary

Atmospheric oscillations with periods up to several 100 years exist at altitudes up to 110 km. They are also seen in computer models (GCM) of the atmosphere. They are often attributed to external influences from the sun, from the oceans, or from atmospheric constituents. This is difficult to verify as the atmosphere cannot be manipulated in an experiment. However, a GCM can be changed arbitrarily! Doing so we find that long period oscillations **may** be excited internally in the atmosphere.

102
103 Multi-annual oscillations with periods between 2 and 11 years have frequently been discussed
104 for the atmosphere and the ocean. Major examples are the Quasi-Biennial Oscillation (QBO),
105 solar cycle related variations near 11 years and 5.5 years, and the El Nino/Southern
106 Oscillation (ENSO). (For references see for instance Offermann et al., 2015.)

107 Self-excited oscillations in the ocean of such periods have been described for instance by
108 White and Liu (2008). Self-excited oscillations in the atmosphere with periods between 2.2
109 and 5.5 yr have been shown in a large altitude regime by Offermann et al. (2015). Their
110 periods are surprisingly robust, i.e. there is little change with altitude. They are also present in
111 general circulation models, the boundaries of which are kept constant.

112 Oscillations of much longer periods in the atmosphere and the ocean have also been
113 reported. Biondi et al. (2001) found bi-decadal oscillations in local tree ring records that date
114 back several centuries. Kalicinsky et al. (2016, 2018) recently presented a temperature
115 oscillation near the mesopause with a period near 25 years which may be interpreted as a self-
116 excited oscillation. Low-frequency oscillations (LFO) on local and global scales in the multi-
117 decadal range (50-80 yr) have been discussed several times (e.g., Schlesinger and Ramankutty
118 (1994); Minobe (1997); Polyakov et al.(2003); Dai et al.(2015); Dijkstra et al.(2005)). Some
119 of these results were intensively discussed as internal variability of the atmosphere-ocean
120 system, for instance as the internal interdecadal modes AMV (Atlantic Multidecadal
121 Variability) and PDO/IPO (Pacific Decadal Oscillation/Interdecadal Pacific Oscillation) (e.g.
122 Meehl et al., 2013; 2016; Lu et al., 2014; Deser et al., 2014; Dai et al., 2015.) Multidecadal
123 variations (40-80 years) of Arctic-wide surface air temperatures were, however, related to
124 solar variability by Soon (2005). Some of these long period variations have been traced
125 backwards for two or more centuries (Minobe, 1997; Biondi et al., 2001; Mantua and Hare,
126 2002; Gray et al., 2004). Multidecadal oscillations have also been discussed extensively as
127 internal climatic variability in the context of the long term climate change (temperature
128 increase) in the IPCC AR5 Report (e.g. Flato et al., 2013).

129 Even longer periods of oscillations in the ocean and the atmosphere have also been
130 reported. Karneckas et al. (2012) find centennial variations in three general circulation
131 models of the ocean. These variations occur in the absence of external forcing, i.e. they show
132 internal variabilities on the centennial time scale. Internal variability in the ocean on a
133 centennial scale is also discussed by Latif et al. (2013) on the basis of model simulations.
134 Measured data of a 500 year quasi-periodic temperature variation are shown by Xu et al.
135 (2014). They analyze a more than 5000 year long pollen record in East Asia. Very long
136 periods are found by Paul and Schulz (2002) in a climate model. They obtain internal
137 oscillations with periods of 1600-2000 years.

138 All long period oscillations cited here refer to temperatures of the ocean or the land/ocean
139 system. It is emphasized that on the contrary the self-excited multi-annual oscillations
140 described by Offermann et al. (2015) and those discussed in the present paper are properties
141 of the atmosphere, and exist in a large altitude regime between the ground and 110 km
142 altitude. They are not related to the ocean (see below).

143 In the present paper the work of Offermann et al. (2015) is extended to multi-decadal and
144 centennial periods. Internal oscillations in the atmosphere are studied in three general
145 circulation models. The analysis is locally constrained (Central Europe), but vertically
146 extended up to 110 km. The model boundary conditions (sun, ocean, trace gases) are kept
147 constant. The results of model runs with HAMMONIA, WACCM, and ECHAM6 were made
148 available to us. They simulate 34 years, 150 years, and 400 years of atmospheric behavior,
149 respectively. The corresponding results are compared to each other. Most of the analyses are
150 performed for atmospheric temperatures.

151 For comparison, long duration measured data series are also analyzed. There is a data set
152 taken at the Hohenpeißenberg Observatory (47.8°N, 11.0°E) since 1783. Long term data have

153 been globally averaged by Hansen et al., (2010), and published as GLOTI data (Global Land
154 Ocean Temperature Index).

155 In Section 2 of this paper the three models are described and the analysis method is
156 presented. In Section 3 the oscillations obtained from the three models are compared. The
157 vertical structures of the periods, amplitudes, and phases of the self-excited oscillations are
158 described. In Section 4 the results are discussed. Section 5 gives a summary and some
159 conclusions.

160

161

162

163 2 Model data and their analysis

164

165

166 2.1 Self-excited oscillations and their vertical structures

167

168 In an earlier paper (Offermann et al., 2015) multi-annual oscillations with periods of about
169 2 - 5 years have been described at altitudes up to 110 km. These were found in temperature
170 data of HAMMONIA model runs (see below). They were present in the model even if the
171 model boundary conditions (solar irradiance, sea-surface temperatures and sea ice, boundary
172 values of green-house gases) were kept constant. Therefore they were interpreted as self-
173 excited oscillations. The periods were found to be quite robust as they did not change much
174 with altitude. The oscillations showed particular vertical structures of amplitudes and phases.
175 Amplitudes did not increase exponentially with altitude as they do with atmospheric waves.
176 They rather varied with altitude between maximum and near zero values in a nearly regular
177 manner. Phases showed jumps of about 180° at the altitudes of the amplitude minima, and
178 were about constant in between. There were indications of synchronization of amplitudes and
179 phases.

180 The periods analyzed in the earlier paper have been restricted to below 5.5 yr. Much longer
181 periods have been described in the literature. It is therefore of interest to see whether such
182 longer periods could also be self-excited in the models, and what their origin might be.

183 Figure 1 shows an example of such temperature structures for an oscillation with a period
184 of 17.3 ± 0.8 years obtained from the HAMMONIA model discussed below. This picture is
185 typical of the oscillations in Offermann et al. (2015) and of the oscillations discussed in the
186 present paper. The periods at the various altitudes are close to their mean value even though
187 the error bars are fairly large. There is no indication of systematic altitude variations, and
188 therefore the mean is taken as a first approximation. At some altitudes the periods could not
189 be determined (see Section 3.3). In these cases the periods were prescribed by the mean of the
190 derived periods (dash-dotted red vertical line, 17.3 yr) to obtain approximate amplitudes and
191 phases at these altitudes (see Offermann et al., 2015). Details of the derivation of periods,
192 amplitudes, and phases are given in Section 3.2, Lines 447pp.

193

194

195 2.2 HAMMONIA

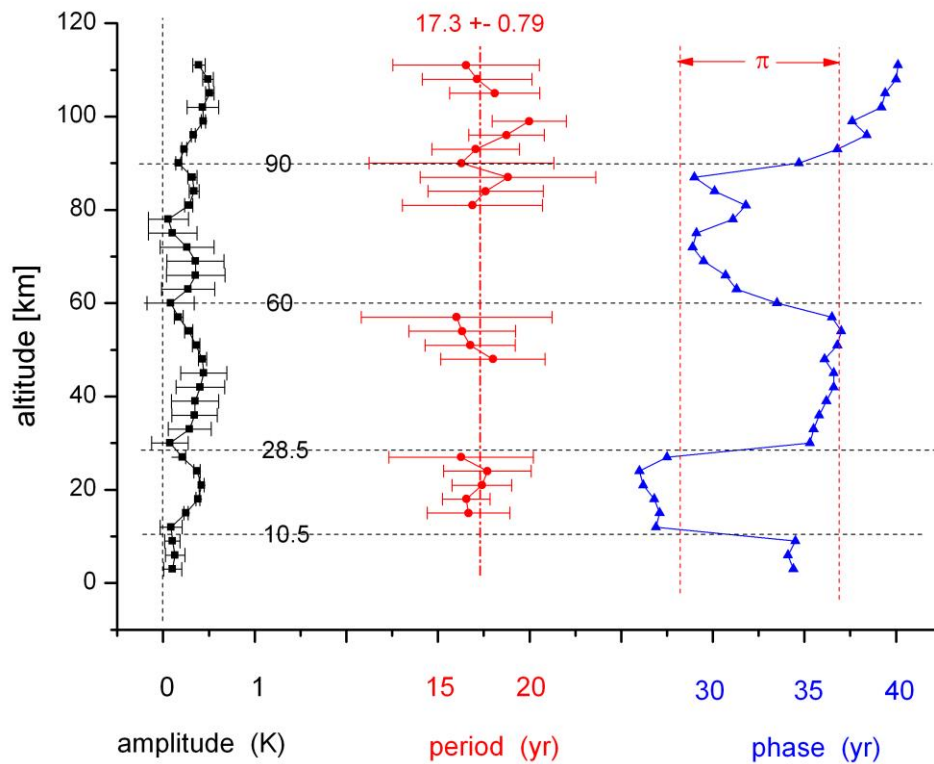
196

197 The HAMMONIA model (Schmidt et al., 2006) is based on the ECHAM5 general circulation
198 model (Röckner et al., 2006), but extends the domain vertically to 2×10^{-7} hPa, and is coupled
199 to the MOZART3 chemistry scheme (Kinnison et al., 2007). The simulation analyzed here
200 was run at a spectral resolution of T31 with 119 vertical layers. The relatively high

201

202

203



204
205

206 Fig. 1 Vertical structures of self-excited oscillation periods near 17.3 ± 0.8 yr from
207 HAMMONIA temperatures.
208 Missing period values could not be derived from the data. They were prescribed as the mean
209 value 17.3 yr (dash-dotted vertical red line, see text and Section 3.2). Phases are relative
210 values.

211
212 vertical resolution of less than 1 km in the stratosphere allows an internal generation of the
213 QBO. Here we analyze the simulation (with fixed boundary conditions, including aerosol,
214 ozone climatology) that was called “Hhi-max” in Offermann et al. (2015), but instead of only
215 11 we use 34 simulated years. Further details of the simulation are given by Schmidt et al.
216 (2010).

217 *As concerns the land parameters part of them were also kept constant (vegetation*
218 *parameters as leaf area, wood coverage) and ground albedo. Others were not*
219 *(e.g. snow and ice on lakes). Hence, some corresponding small (?) influence on our*
220 *oscillations cannot be excluded.*

221 An example of the HAMMONIA data is given in Fig. 2 for 0 km and 3 km altitudes. The
222 HAMMONIA data were searched for self-excited oscillations up to 110 km. The detailed
223 analysis is described below (Section 3.2). Nine oscillations were identified with periods
224 between 5.3 yr and 28.5 yr. They are listed in Table 2a. The oscillation shown in Fig. 1 (17.3
225 yr) is from about the middle of this range.

226
227
228
229
230
231
232

2.3 WACCM

233
234
235
236
237
238
239
240
241
242
243
244
245
246
247
248
249
250
251
252
253
254
255
256
257
258
259
260
261
262
263
264
265
266
267
268
269
270
271
272
273
274
275
276
277
278
279
280
281
282

Long runs with chemistry-climate models (CCMs) having restricted boundary conditions are not frequently available. A model run much longer than 34 years became available from the CESM-WACCM4 model. This 150 year run was analyzed from the ground up to 108 km. The model experiments are described in Hansen et al. (2014). Here, the experiment with monthly varying constant climatological SSTs and sea ice has been used, i.e., there is a seasonal variation, but it is the same in all years. Other boundary conditions such as Greenhouse Gases (GHG) and Ozone Depleting Substances (ODP) were kept constant at 1960 values.

Solar cycle variability, however, was not kept constant during this model experiment. Spectrally resolved solar irradiance variability as well as variations of the total solar irradiance and the F10.7cm solar radio flux were used from 1955 to 2004 from Lean et al. (2005). Thereafter solar variations from 1962-2004 were used as a block of proxy data and added to the data series several times to reach 150 years in total. Details are given in Matthes et al. (2013).

The WACCM data were analyzed for self-excited oscillations in the same manner as the HAMMONIA data. Here, the emphasis is on longer periods. Besides many shorter oscillations, nine oscillations with periods of more than 20 years were found. These results are included to Table 2a.

2.4 ECHAM6

The longest computer run available to us, covering 400 years, is from ECHAM6. ECHAM6 (Stevens et al., 2013) is the successor of ECHAM5, the base model of HAMMONIA. Major changes relative to ECHAM5 include an improved representation of radiative transfer in the solar part of the spectrum, a new description of atmospheric aerosol, and a new representation of the surface albedo. While the standard configuration of ECHAM5 used a model top at 10 hPa, this was extended to 0.01 hPa in ECHAM6. As the atmospheric component of the Max-Planck-Institute Earth System Model (MPI-ESM, Giorgetta et al., 2013) it has been used in a large number of model intercomparison studies related to the Coupled Model Intercomparison Project phase 5 (CMIP5). The ECHAM6 simulation analyzed here was run at T63 spectral resolution with 47 vertical layers (not allowing for an internal generation of the QBO). All boundary conditions were fixed to constant values, taken as an average of the years 1979 to 2008.

The temperature data were analyzed as the other data sets described above. Seventeen oscillation periods longer than 20 yr were obtained (Table 2a), with the typical vertical structures of self-excited oscillations. The ECHAM6 results in this paper are considered an approximate extension of the HAMMONIA results.

A summary of the model properties is given in Table 1. All analyses in this paper are for Central Europe. The vertical model profiles are for 50°N, 7°E.

3 Model results

3.1 Vertical correlations of atmospheric temperatures

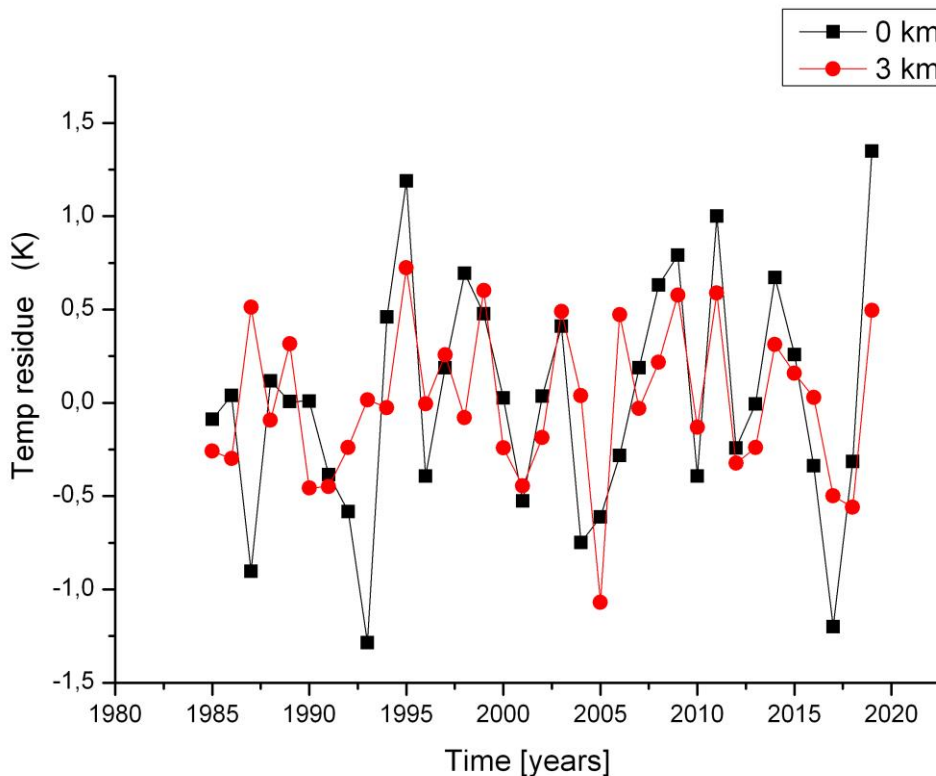
283 Figure 1 indicates that there are some vertical correlation structures in the atmospheric
284 temperatures. This was studied in detail for the HAMMONIA and ECHAM6 data.

285 Ground temperature residues from the HAMMONIA run 38123 (34 years) are shown in
286 Fig. 2 (black squares). The mean temperature is 281.89 K, which was subtracted from the
287 model data. The boundary conditions (sun, ocean, green house gases, soil humidity, land use,
288 vegetation) have been kept constant, as discussed above. The temperature fluctuations thus
289 show the atmospheric variability (standard deviation is $\sigma = 0.62$ K). This variability is
290 frequently termed “(climate) noise” in the literature. It will be checked whether this notion is
291 justified in the present case.

292 Also shown in Fig. 2 are the corresponding HAMMONIA data for 3 km altitude. The mean
293 temperature is 266.04 K, the standard deviation is $\sigma = 0.41$ K. The statistical error of these
294 two standard deviations is about 12%. Hence the internal variances at the two altitudes are
295 statistically different. This suggests that there may be a vertical structure in the variability that
296 should be analyzed.

297 The data sets in Fig. 2 show large changes within short times (2-4 years). Sometimes these
298 changes are similar at the two altitudes. The variability of HAMMONIA thus appears to
299 contain an appreciable high frequency component and thus needs to be analyzed as well for
300 vertical as for spectral structures.

301
302



303
304

305 Fig. 2 HAMMONIA temperature residues at 0 km and 3 km altitude with fixed boundary
306 conditions (see text). Mean temperatures of 281.89 K (0 km) and 266.04 K (3 km) have been
307 subtracted from the model temperatures. Data are for 50°N, 7°E.

308

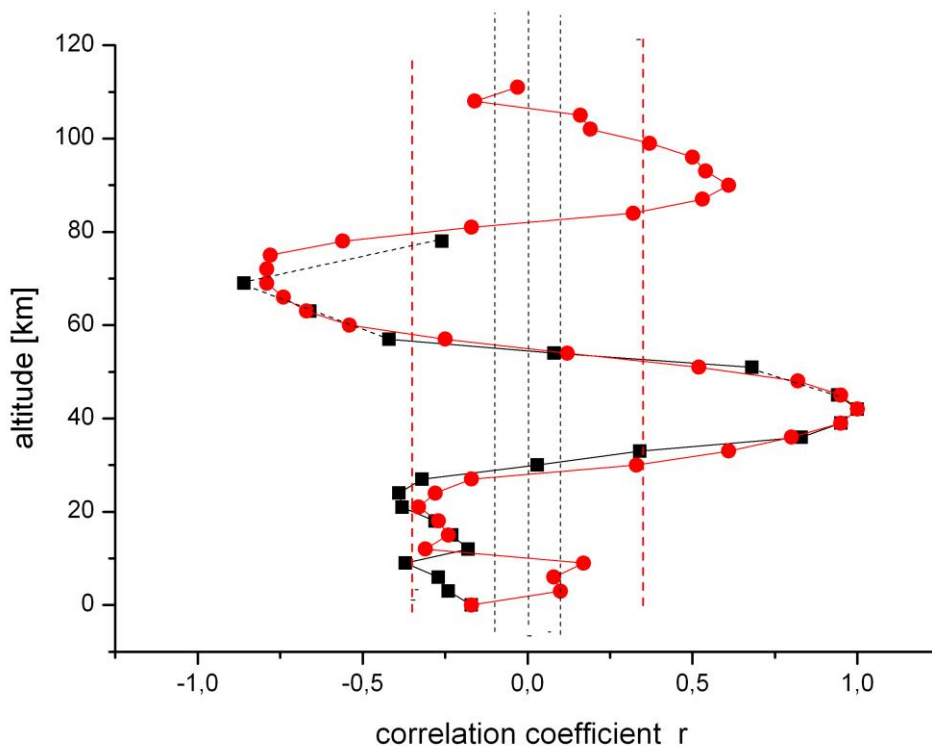
309 Temperatures at layers 3 km apart in altitude were therefore correlated with those at 42 km as
310 a reference altitude (near stratopause). The results are shown in Fig. 3 for the HAMMONIA
311 model run up to 105 km (red dots). A corresponding analysis for the much longer model run

312 of ECHAM6 is also shown (black squares, up to 78 km). Two important results are obtained:
 313 1) There is an oscillatory vertical structure in the correlation coefficient r with a maximum in
 314 the upper mesosphere/lower thermosphere, and two minima in the lower stratosphere and in
 315 the mesosphere, respectively (for HAMMONIA). The correlations are highly significant near
 316 the upper three of these extrema (see the 95% lines in Fig. 3). 2) The correlations in the two
 317 different data sets are nearly the same above the troposphere. This is remarkable because the
 318 two sets cover time intervals very different in length (34 years vs 400 years, respectively).
 319 Therefore, the correlation structure appears to be a basic property of the atmosphere (see
 320 below).

321 The correlations suggest that the fluctuations in the atmosphere (or part of them) are
 322 somehow “synchronized” at adjacent altitude levels. A vertical (layered) structure might
 323 therefore be present in the magnitude of the fluctuations, too. This was studied by means of
 324 the standard deviations σ of the temperatures T , the result is shown in Fig. 4. There is indeed a
 325 vertical structure with fairly pronounced layers.

326 The HAMMONIA data used for Fig. 4 were annual data that have been smoothed by a four
 327 point running mean. This was done to reduce the influence of high frequency “noise”
 328 mentioned above, which is substantial (a factor of 2). The correlation calculations were
 329 repeated with the unsmoothed data. The results are essentially the same. The same applies to
 330 the standard deviations.

331 The layered structures shown in Fig. 3 and 4 are not unrelated. This can be seen in Fig. 4
 332 that also gives the vertical correlations r (Fig. 3) for comparison. The horizontal dashed lines
 333 indicate that the maxima of the standard deviations occur near the extrema of the correlation
 334 profile in the stratosphere and lower mesosphere. This suggests that the fluctuations in
 335 adjacent σ maxima (and in adjacent layers) are anticorrelated. Surprisingly these
 336 anticorrelations are also approximately seen in the amplitude and phase profiles of Fig.1 that
 337 are typical of all oscillations (see below).
 338



339
 340

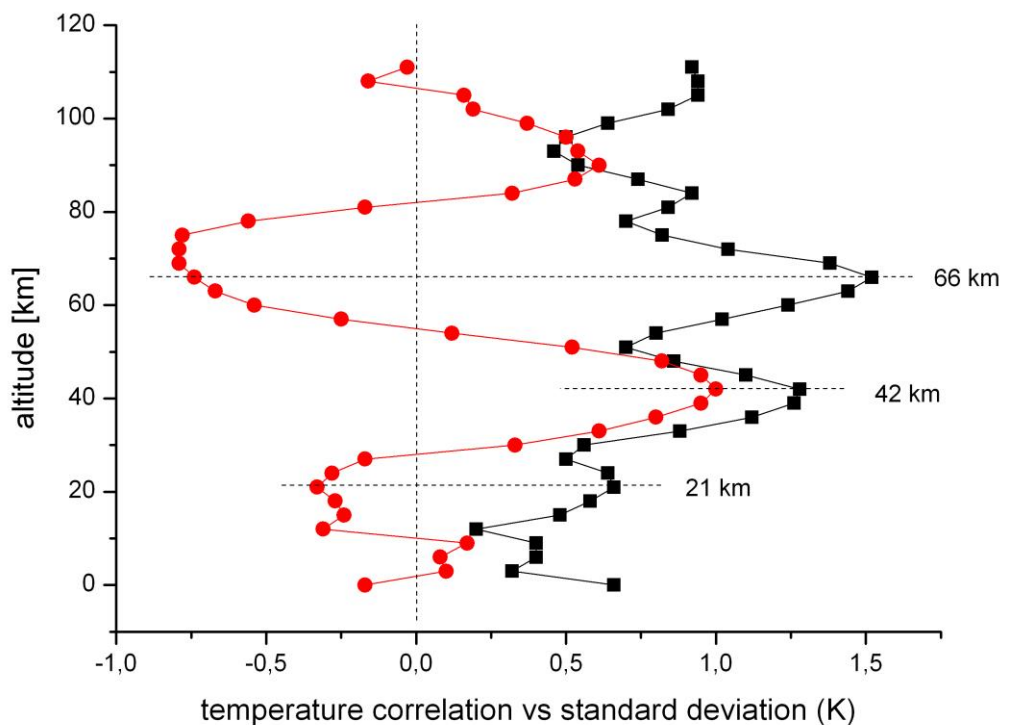
341 Fig. 3 Vertical correlation of temperatures in HAMMONIA (red dots) and ECHAM6 (black
 342 squares). Reference altitude is 42 km ($r = 1$). Vertical dashed lines show 95% significance for
 343 HAMMONIA (red) and ECHAM6 (black).

344
 345

346 The ECHAM6 data have been analyzed in the same way as the HAMMONIA data,
 347 including a smoothing by a 4 point running mean. The data cover the altitude range of 0
 348 -78 km for a 400 year simulation. The results are very similar to those of
 349 HAMMONIA. This is shown in Fig. 5 that gives vertical profiles of standard deviations and
 350 of vertical correlations of the smoothed ECHAM6 data, and is to be compared to the
 351 HAMMONIA results in Fig. 4. The two upper maxima of standard deviations are again
 352 anticorrelated.

353 It is apparently a basic property of the atmosphere's internal variability to be organized in
 354 some kind of "layers", and that adjacent layers are anti-correlated. It appears therefore
 355 questionable whether the internal variability may be termed "noise", as is frequently done in
 356 the literature.

357
 358



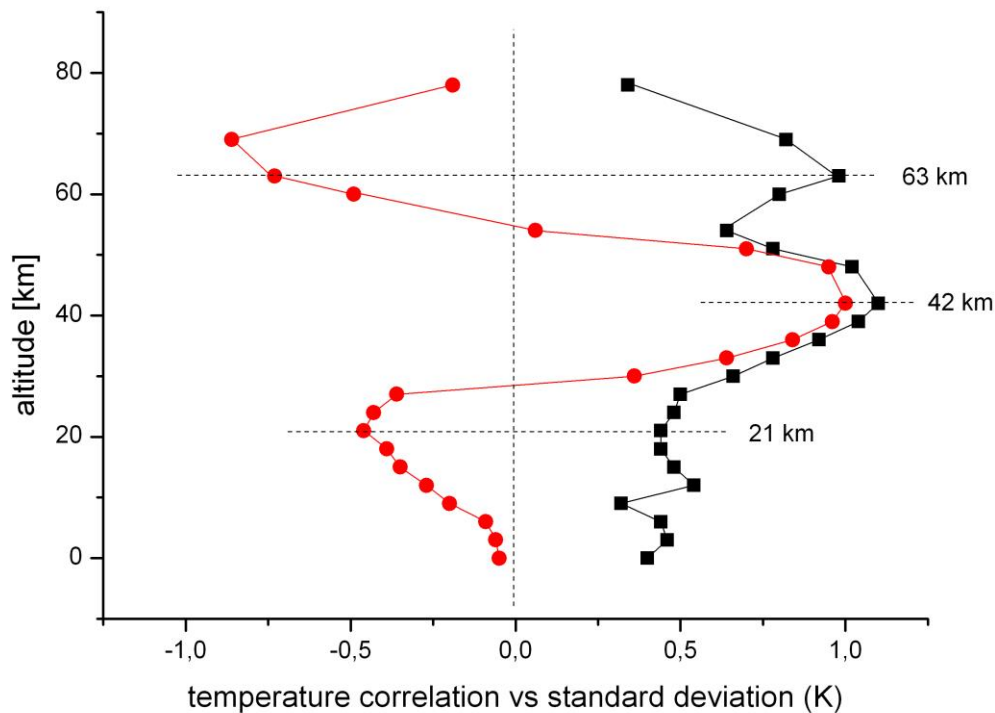
359
 360

361 Fig. 4 HAMMONIA temperatures: Comparison of standard deviations (black squares,
 362 multiplied by 2 for easier comparison) and correlation coefficients (red dots, see Fig. 3). For
 363 details see text.

364
 365
 366
 367
 368
 369

370 3.2 Time structures

371
372 The correlations/anticorrelations concern temporal variations of temperatures. This suggests
373 a search for some kind of regular (ordered) structure in the time series, as well. Therefore in a
374 first step, FFT analyses have been performed for all HAMMONIA altitude levels (3 km
375 apart). The results are shown in Fig. 6 that gives amplitudes for the period range of 4 - 34
376 years versus altitude. Also in this picture, the amplitudes show a layered structure. In addition
377 an ordered structure in the period domain is also indicated. There are increased or high
378 amplitudes near certain period values, for instance at the left and right hand side and in the
379 middle of the picture. A similar result is obtained for the ECHAM6 data shown in Fig. 7 for
380 the longer periods of 10-400 years. The layered structure in altitude is clearly seen, and so are
381 the increased amplitudes near certain period values. Obviously, the computer simulations
382 contain periodic temperature oscillations, the amplitudes of which show a vertically layered
383 order. Because **most** boundary conditions of the computer runs were kept constant, these
384 oscillations **hardly** be excited from the outside. They are therefore interpreted as self-excited
385 oscillations, and thus as intrinsic properties of the atmosphere
386
387
388



389 Fig. 5 ECHAM6 temperatures: Comparison of standard deviations (black squares,
390 multiplied by 2) and correlation coefficients (red dots). For details see text.
391
392

393
394 The amplitudes shown in Fig. 6 and 7 are relative values, and the resolution of the spectra is
395 quite limited. Therefore a more detailed analysis is required. For this purpose the Lomb-
396 Scargle Periodogram (Lomb 1976; Scargle 1982) is used. As an example Fig. 8 shows the
397 mean Lomb-Scargle Periodogram in the period range 20 – 100 years for the ECHAM6 data.
398 For this picture Lomb-Scargle spectra were calculated for all ECHAM6 layers separately, and

399 the mean spectrum of all altitudes was determined. The power of the periodogram gives the
400 reduction in sum of squares when fitting a sinusoid to the data (Scargle, 1982), i.e. it is
401 equivalent to a harmonic analysis using least square fitting of sinusoids. The power values are
402 normalized by the variance of the data to obtain comparability of the layers with different
403 variance. Quite a number of spectral peaks are seen between 20 and 60 years period. Further
404 oscillations appear to be present around 100 years and at even longer periods (not shown here
405 as they are not sufficiently resolved).

406 We compared the mean result for the ECHAM6 data with 10000 representations of noise.
407 One representation covers 47 atmospheric layers. For each representation we took noise from
408 a Gaussian distribution for each atmospheric layer independently, and calculated a mean
409 Lomb-Scargle Periodogram for every representation in the same way as for the ECHAM6
410 data.

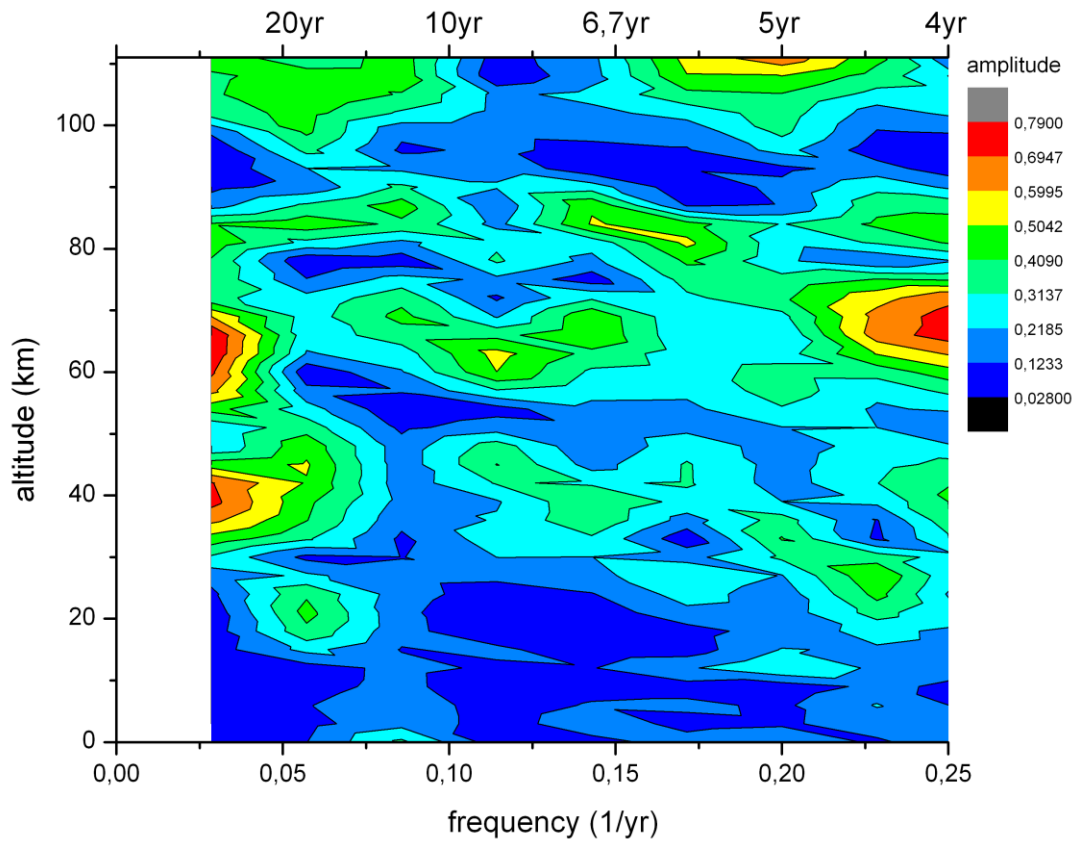
411 It might be considered appropriate to use red noise instead of white noise in this analysis.
412 We therefore calculated the sample autocorrelation at a lag of 1 year for the different
413 ECHAM6 altitudes. These values were found to be very close to zero and, thus, we used
414 Gaussian noise in our analysis.

415 The red line in Fig. 8 shows the average of all of these mean periodograms. As expected for
416 the average of all representations the peaks cancel, and one gets an approximately constant
417 value for all periods. A single representation typically shows one or several peaks above this
418 mean level. The red dashed line gives the upper 2σ level, i.e. the mean plus 2σ . As the mean
419 Lomb-Scargle Periodogram for the ECHAM6 data shows several peaks clearly above this
420 upper 2σ level, this mean periodogram is significantly different from that of independent
421 noise. Therefore, the conclusion is that independent noise at the different atmospheric layers
422 alone cannot explain the observed periodogram showing large remaining peaks after
423 averaging.

424 The period values shown in Fig. 8 agree with those given for ECHAM6 in Table 2a which
425 are from the harmonic analysis described next. The agreement is within the error bars given in
426 Table 2a (except for 24.3).

427 A spectral analysis as that in Fig. 8 was also performed for the HAMMONIA temperatures.
428 It showed the periods of 5.3 yr and 17.3 yr above the 2σ level. These values agree within
429 single error bars with those given in Table 2a. All peaks found to be significant (in different
430 analyses) are marked by heavy print in Table 2a.

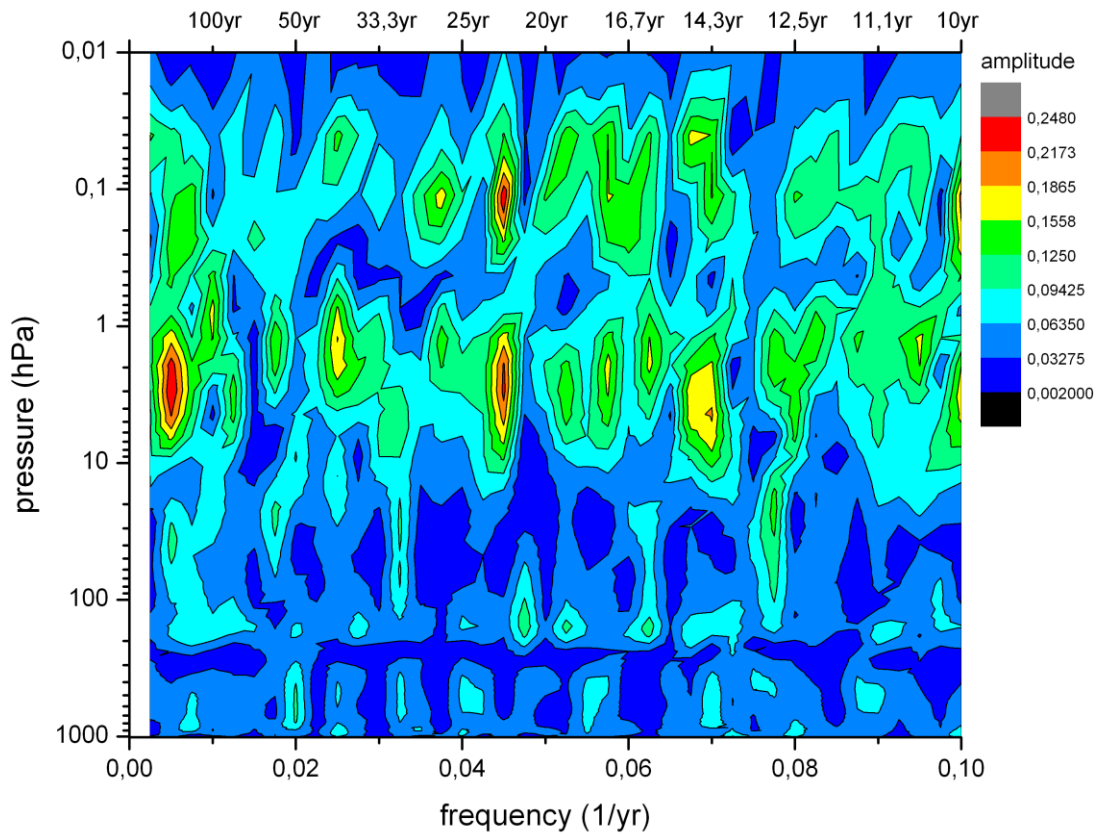
431



432
 433 Fig. 6 Self-excited temperature oscillations in the HAMMONIA model.
 434 FFT amplitudes are shown in dependence on altitude and frequency (periods 4 – 34 yr).
 435 Colour code of amplitudes is in arbitrary units.

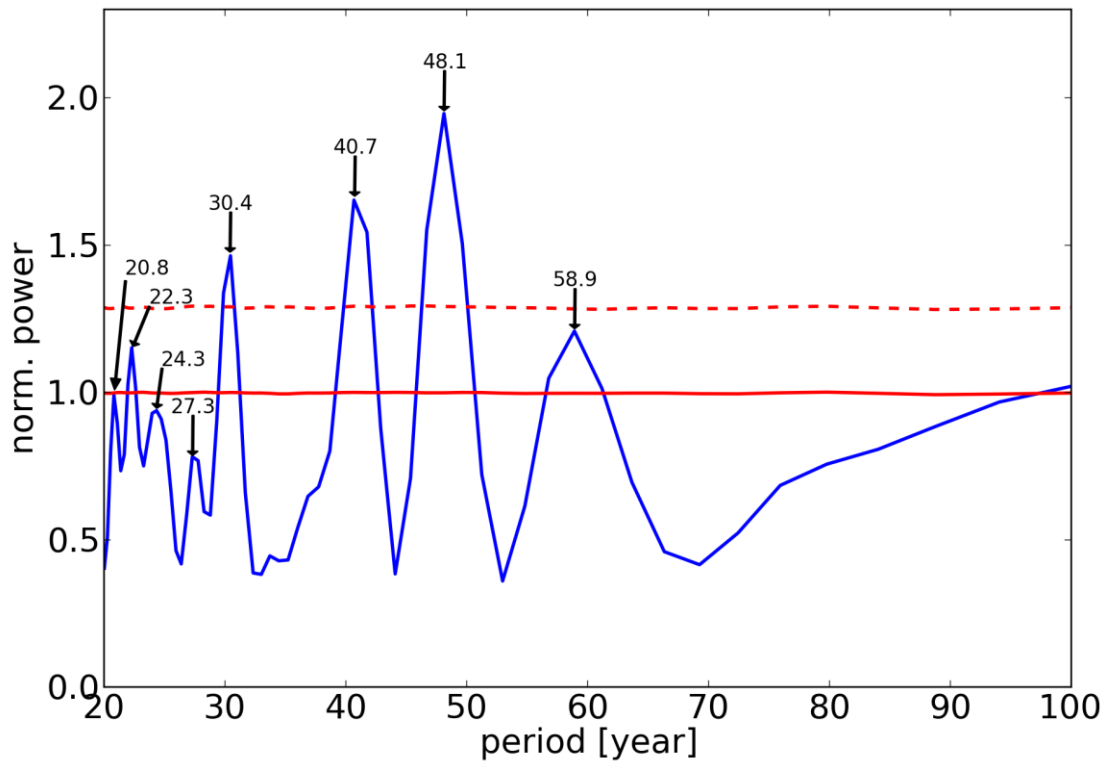
436
 437
 438 The Lomb-Scargle spectra (in their original form) do not reveal the phases of the
 439 oscillations. We have therefore added harmonic analyses to our data series. This was done
 440 by stepping through the period domain in steps 10% apart. In each step we looked for the
 441 largest near-by sinus oscillation peak. This was done by means of an ORIGIN search
 442 algorithm (ORIGIN Pro 8G, Levenberg-Marquardt algorithm) that yielded optimum values
 443 for period, amplitude, and phase. The algorithm starts from a given initial period and looks for
 444 a major oscillation in its vicinity. For this it determines period, amplitude, and phase,
 445 including error bars. If in this paper the term “harmonic analysis” is used, this algorithm is
 446 always meant. The results are a first approximation, though, because only one period was
 447 fitted at a time, instead of the whole spectrum. Furthermore, the 10% grid may be sometimes
 448 too coarse. Also small amplitude oscillations may be overlooked.

449
 450
 451
 452



453
 454
 455
 456
 457
 458

Fig. 7 Self-excited temperature oscillations in the ECHAM6 model. FFT amplitudes are shown in dependence on altitude and frequency (periods 10 – 400 yr). Colour code of amplitudes is in arbitrary units.



459

460
461
462
463

Fig. 8 Self-excited temperature oscillations in the ECHAM6 model
Lomb-Scargle periodogram is given for periods of 20 – 100 years. Dashed red line indicates
significance at the 2σ level. For straight red line see text.

464

465

466 This analysis was performed for all altitude levels available. Figure 1 shows an example for
467 the HAMMONIA temperatures from 3-111 km for periods around 15 – 20 years. The middle
468 track (red dots) shows the periods with their error bars, the left side shows the amplitudes, and
469 the right side the phases. The mean of all periods is 17.3 ± 0.79 years. There are several
470 altitudes where the harmonic analysis does not give a period. This may occur if an amplitude
471 is very small or if there is a near-by period with a strong amplitude that masks the smaller
472 one. At these altitudes the periods were interpolated for the fit (dash-dotted vertical line). The
473 mean of the derived periods (17.3 yr) is used as an estimated interpolation value. This is
474 because the derived periods do not deviate too much from the mean value. This procedure
475 allows to obtain estimated amplitude and phase values for instance in the vicinity of the
476 amplitude minima. That is important because at these altitudes large phase changes are
477 frequently observed. The Levenberg-Marquardt algorithm calculates an amplitude and phase
478 if a prescribed (estimated) period is provided.

479

480 The right track in Fig. 1 shows the phases of the oscillations. The special feature about this
481 vertical profile is its steplike structure with almost constant values in some altitudes and a
482 subsequent fast change somewhat higher to some other constant level. These changes are by
483 about 180° (π), i.e. the temperatures above and below these levels are anti-correlated. At these
484 levels the temperature amplitudes (left track) are minimum, with maxima in between. These
485 maxima occur near the altitudes of the maxima of the temperature standard deviations in Fig.
486 4 that are anti-correlated in adjacent layers. The phase steps in Fig. 1 approximately fit to this
487 picture. They suggest that the layer anti-correlation discussed above corresponds at least in
488 part to the phase structure of the self-excited oscillations in the atmosphere.

488

489 This important result was checked by an analysis of other oscillations contained in the
490 HAMMONIA data series. Nine self-excited oscillations with periods between 5.34 years and
491 28.5 years were obtained by the analysis procedure described above. They are listed in Table
492 2a, and all show vertical profiles similarly as in Fig. 1.

492

493 Figure 1 shows that at different altitudes the periods are somewhat different. They cluster,
494 however, quite closely about their mean value of 17.3 yr. This clustering about a mean value
495 is found for almost all periods listed in Table 2a. This is shown in detail in Fig. 9 and 10
496 which give the number of periods found at different altitudes in a fixed period interval. The
497 clusters are separated by major gaps, as is indicated by vertical dashed lines (black). This
498 suggests to use a mean period value as an estimate of the oscillation period representative for
499 all altitudes. The mean period values are given above each cluster in red, together with a red
500 solid line. A few clusters are not very pronounced, and hence the corresponding mean
501 period values are unreliable (e.g. those beyond 20 yr, see the increased standard deviations in
502 Table 2a).

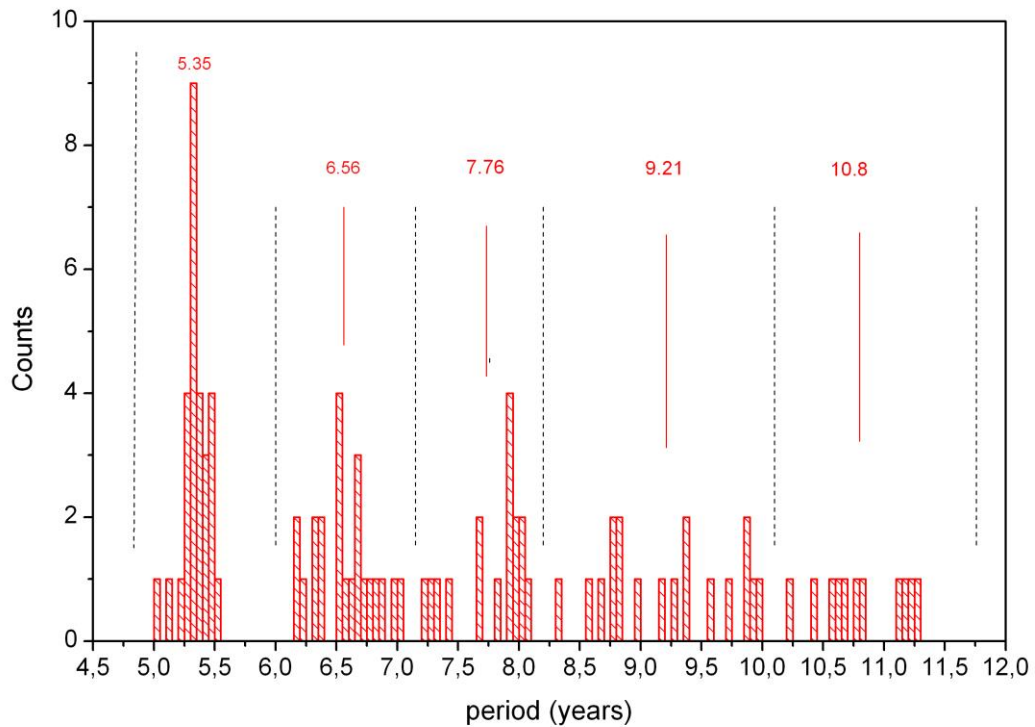
502

503 In determining the mean oscillation periods we have avoided subjective influences as
504 follows: Periods obtained at various altitudes were plotted versus altitude as shown in Fig. 1
505 (middle column, red). When covering the period range 5 to 30 years nine vertical columns
506 appeared. The definition criterion of the columns was that there should not be any overlap
507 between adjacent columns. It turned out that such an attribution was possible. To make this
508 visible we have plotted the histograms in Fig. 9 and 10. The pictures show that the column
509 values form the clusters mentioned which are separated by gaps. The gaps that are the largest
ones in the neighbourhood of a peak are used as boundaries (except at 7.15 yr). It turns out

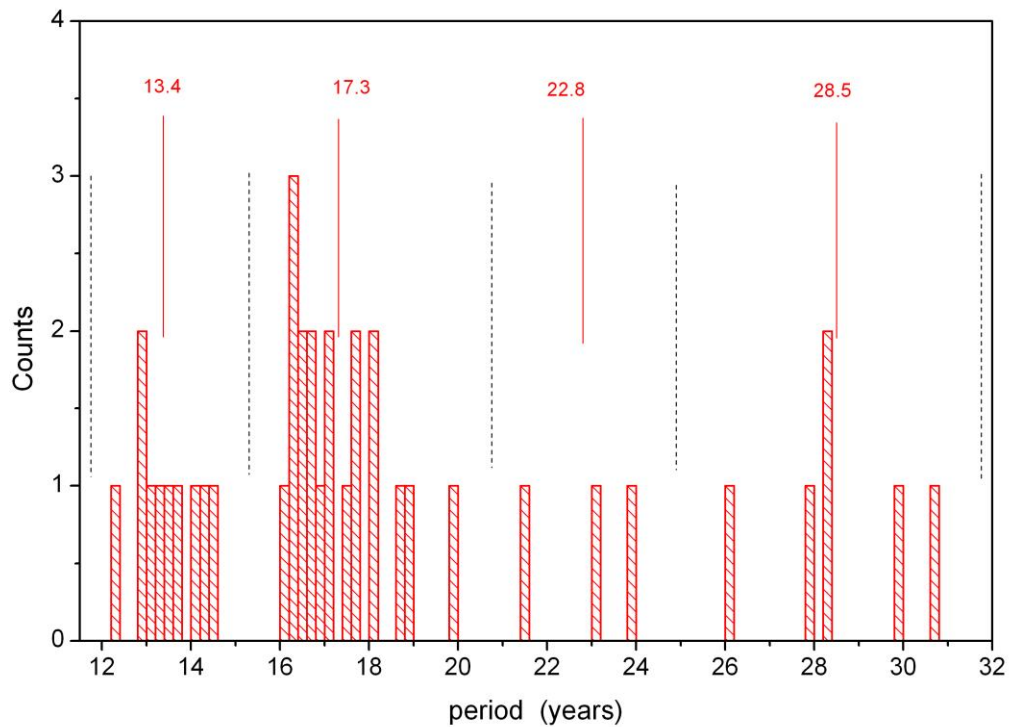
510 that if an oscillation value near to a boundary is tentatively shifted from one cluster to the
 511 neighbouring one the mean cluster values experiences only minor changes. Figure 10 shows
 512 that our procedure comes to its limits, however, for periods longer than 20 years (for
 513 HAMMONIA). This is seen in Tab.2a from the large error bars. We still include these values
 514 for illustration and completeness.

515 It is important to note that all HAMMONIA values in Tab.2a (except 28.5 yr) agree with
 516 the Hohenpeißenberg values within the combined error bars. The Hohenpeißenberg data are
 517 ground values and hence not subject to our clustering procedure. Furthermore also all other
 518 model periods in Tab.2a have been derived by the same cluster procedure. The close
 519 agreement discussed in the text suggests that this technique is reliable.

520
 521 ECHAM6 - data are used in the present paper to analyze much longer time windows (400
 522 years) than that of HAMMONIA (34 years). Results shown in Fig. 3, 5, and 7 are quite
 523 similar to those of HAMMONIA. Harmonic analysis of self-excited oscillation periods was
 524 performed in the same way as for HAMMONIA. Seventeen periods were found longer than
 525 20 years and have been included to Table 2a. Shorter periods are not shown here as that range
 526 is covered by HAMMONIA. The amplitude and phase structures of these are very similar to



527
 528 Fig. 9 Number of oscillations counted in a fixed period interval at periods 4.75 – 11.75
 529 years. Interval is 0.05 years. (HAMMONIA)

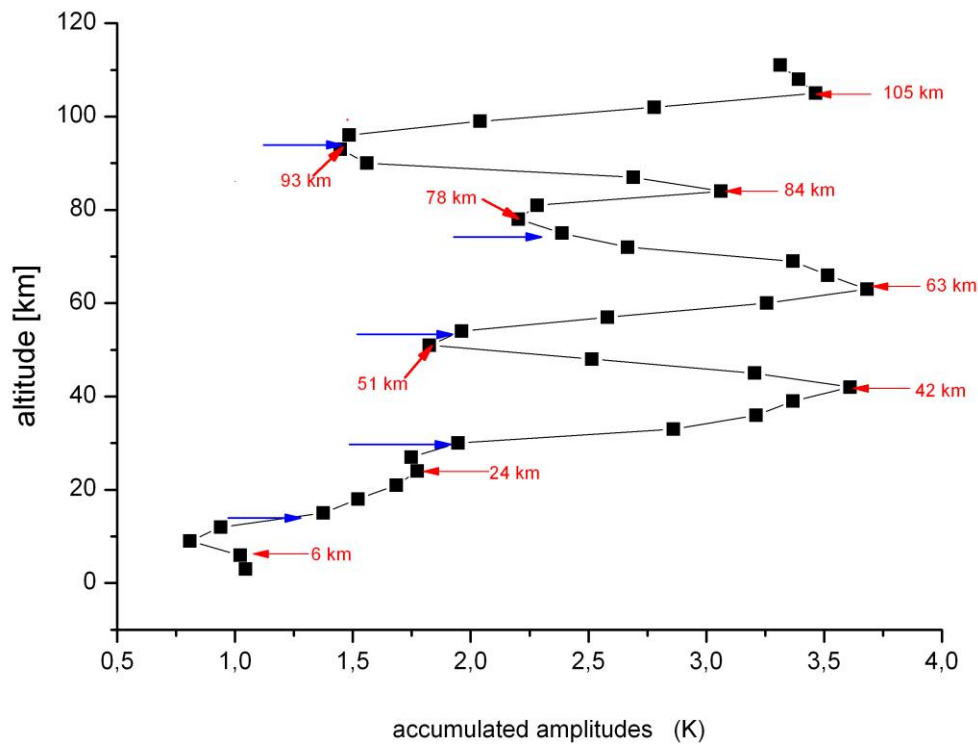


530
 531 Fig. 10 Number of oscillations counted in a fixed period interval at periods 11.75 – 31.75
 532 years. Interval is 0.2 years. (HAMMONIA)
 533

534 those of HAMMONIA. The cluster formation about the mean period values is also obtained
 535 for ECHAM6 and looks quite similar to Fig. 9 and 10.

536 The vertical amplitude and phase profiles of the mean periods given in Table 2a all show
 537 intermittent amplitude maxima/minima, and step-like phase structures. They in general look
 538 very similar to Fig. 1. We have calculated the accumulated amplitudes (sums) from all of
 539 these profiles at all altitudes. They are shown in Fig. 11a for HAMMONIA. They clearly
 540 show a layered structure similar to the temperature standard deviations in Fig. 4, with maxima
 541 at altitudes close to those of the standard deviation maxima. The figure also closely
 542 corresponds to the amplitude distribution shown in Fig. 1, with maxima and minima occurring
 543 at similar altitudes in either picture.

544 Accumulated amplitudes have also been calculated for the ECHAM6 periods, and similar
 545 results are obtained as for HAMMONIA (see Fig. 11b). The similarity is already indicated in
 546 Fig. 3 above 15 km. The correlation of the HAMMONIA and ECHAM6 curves above this
 547 altitude has a correlation coefficient of 0.97. This and Fig. 11 supports the idea that all self-
 548 excited oscillations have a similar vertical amplitude structure



549
550

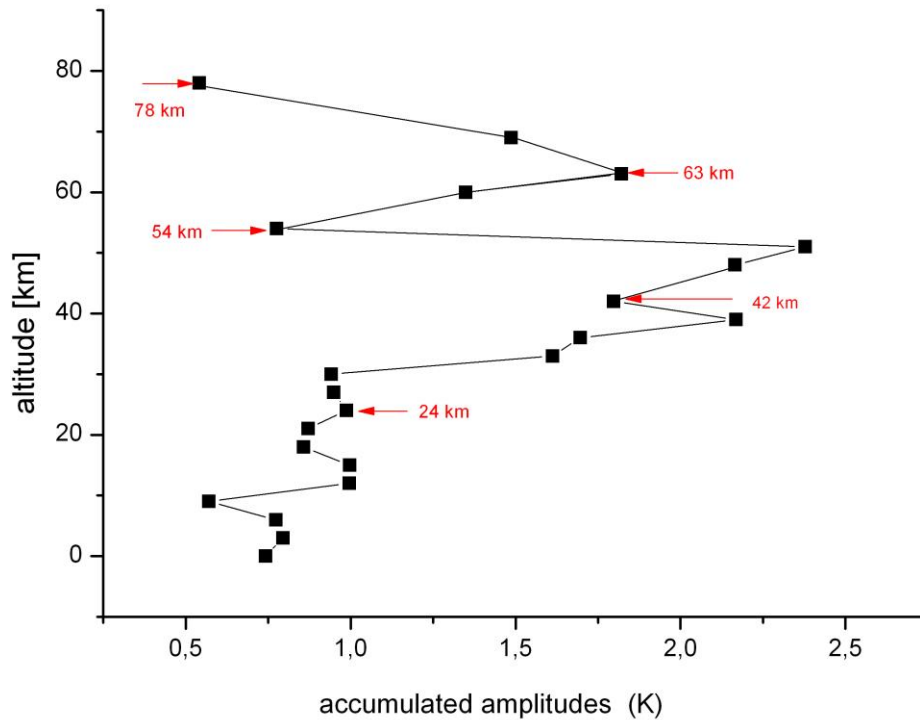
551 Fig. 11a Self-excited temperature oscillations in the HAMMONIA model.
552 Accumulated amplitudes are shown vs altitude for periods of 5.3 – 28.5 years (see Table 2a).
553 Blue horizontal arrows show mean altitudes of phase jumps. Red arrows indicate altitudes of
554 maxima and minima.

555
556

557 The phase jumps in the nine oscillation vertical profiles of HAMMONIA also occur at
558 similar altitudes. Therefore the mean altitudes of these jumps have been calculated and are
559 shown in Fig. 11a as blue horizontal arrows. They are seen to be close to the minima of the
560 accumulated amplitudes and thus confirm the anticorrelations between adjacent layers.
561 Figures 4, 1, and 11 thus show a general structure of temperature correlations/anticorrelations
562 between different layers of the HAMMONIA atmosphere, and suggest the phase structure of
563 the self-excited oscillations as an explanation. The same is valid for ECHAM6.

564 Altogether HAMMONIA and ECHAM6 consistently show the same type of variability and
565 oscillation structures. This type occurs in a wide time domain of 400 years. As mentioned, we
566 do not believe that these ordered structures are adequately described by the term “noise”, as
567 this notion is normally used for something occurring at random.

568
569
570
571



572
573

574 Fig. 11b Self-excited temperature oscillations in the ECHAM6 model
575 Accumulated amplitudes are shown vs altitude for the periods given in Tab. 2a. Red arrows
576 indicate altitudes of maxima and minima.

577
578

579 3.3 Intrinsic oscillation periods

580

581 Three different model runs of different lengths have been investigated by the harmonic
582 analysis described. The HAMMONIA model covered 34 years, the WACCM model covered
583 150 years, and the ECHAM6 model covered 400 years. The intention was to study the
584 differences resulting from the different nature of the models, and from the difference in the
585 length of the model runs.

586

587 The oscillation periods found in these model runs are listed in Table 2a. These periods are
588 vertical mean values as described for Fig. 1 and Figs. 9-10. Periods are given in order of
589 increasing values in years together with their standard deviations. Only periods longer than 5
590 years are shown here. The maximum period cannot be longer than the length of the computer
591 run. Therefore, the number of periods to be found in a model run can -in principle- be the
592 larger the longer the length of the run is. Table 2a shows preferentially periods longer than 20
593 yr (except for HAMMONIA and Hohenpeißenberg) as the emphasis is on the long periods
594 here. Periods comparable to the length of the data series need, of course, be considered with
595 caution.

595

596 The periods shown here at a given altitude are from the Levenberg-Marquardt algorithm (at
597 1σ significance). The values obtained at different altitudes in a given model have been
598 averaged as described above, and the corresponding mean and its standard error is given in
599 Tab.2a.

599

600 Table 2a also contains two columns of periods and their standard deviations that were
derived from *measured* temperatures. These are data obtained on the ground at the

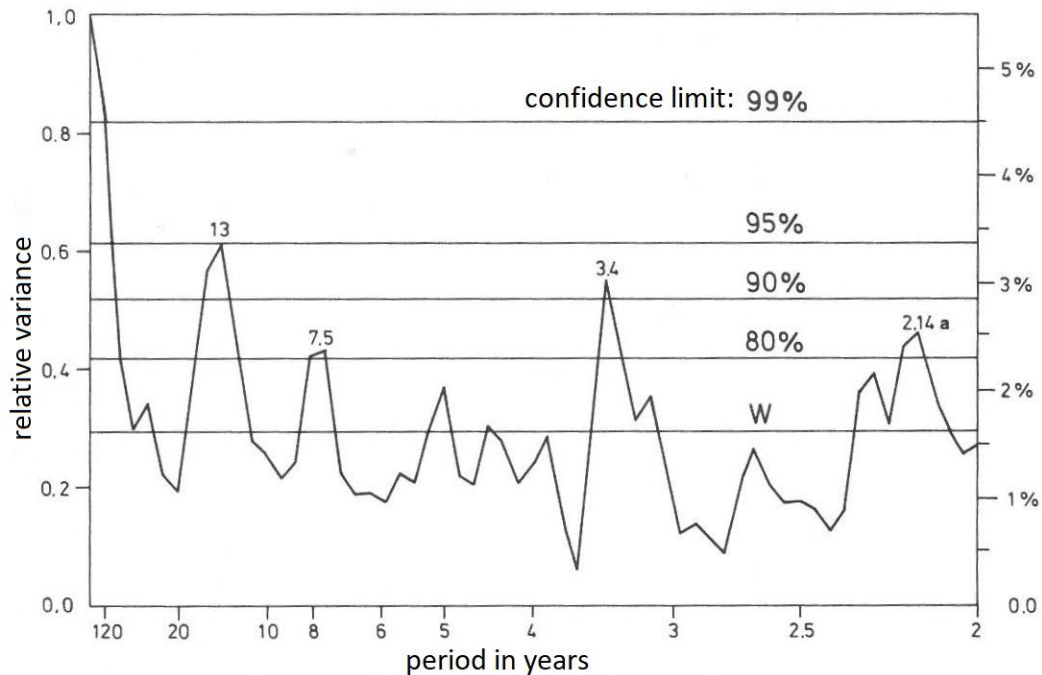
601 Hohenpeißenberg Observatory (47.8°N, 11.0°E) from 1783 to 1980, and globally averaged
602 GLOTI data (Global Land Ocean Temperature Index , Hansen et al., 2010), respectively. The
603 data are annual mean values smoothed by a 16 point running mean and will be discussed
604 below. Data after 1980 are not included in the harmonic analyses because they steeply
605 increase thereafter (“climate change”). The periods are determined as for the data of the other
606 rows of Table 2a (see Section 3.2).

607 The Hohenpeißenberg and GLOTI periods show several close agreements with the
608 HAMMONIA and ECHAM6 results. Further comparisons with other data analyses are given
609 below. A summary is given in Table 2b. Different techniques have been used, such as Single
610 Spectrum Analysis (SSA), Auto correlation Spectral Analysis (ASA), and Detrended
611 Fluctuation Analysis (DFA), and yield similar results. They are also shown in Tab. 2b. For the
612 accuracy and significance of these techniques the reader is referred to the corresponding
613 papers. The periods listed in Tab. 2b are given in bold type in Tab.2a.

614 There are some empty spaces in the lists of Table 2a. It is believed that this is because these
615 oscillations are not excited in that model run, or that their excitation is not strong enough to be
616 detected, or that the spectral resolution of the data series is insufficient (strong changes in
617 amplitudes strengths are, for instance, seen in Fig. 1.). For the *measured* data in Table 2a it
618 needs to be kept in mind that they were under the influence of varying boundary conditions.

619 The model runs shown in Table 2a have different altitude resolutions. The best resolution (1
620 km) is available in HAMMONIA (119 vertical layers, run Hhi-max in the earlier paper of
621 Offermann et al., 2015). The very long run of ECHAM6 uses only 47 layers. Data on a 3 km
622 altitude grid are used here. In the earlier paper it was shown on the basis of a limited data set
623 (HAMMONIA, Hlo-max) that a decrease of the number of layers affected the vertical
624 amplitude and phase profiles of the oscillations found. It did, however, not change the
625 oscillation periods. For a more detailed analysis a 20 year-long run of Hlo-max (67 layers) is
626 now compared to the 34 year- long run of Hhi-max (119 layers). The resulting oscillation
627 periods are shown in Table 3 (together with their standard deviations). Sixteen pairs of
628 periods are listed that all agree within the single error bars (except No. 4). Hence it is
629 confirmed that the periods of the oscillations are quite robust with respect to changes in
630 altitude resolution. The periods of the ECHAM6 run can therefore be considered as reliable,
631 despite their limited altitude resolution.

632
633
634
635



636
 637 Fig. 12 Periodogram (2 yr to 120 yr) of measured Hohenpeißenberg temperatures from
 638 Schönwiese (1992, Abb. 57). Results are from an autocorrelation spectral analysis ASA.
 639
 640

641 When comparing the periods in Table 2a to each other several surprising agreements are
 642 observed. It turns out that all periods of the HAMMONIA and WACCM models find a
 643 counterpart in the ECHAM6 data (not vice versa). These data pairs always agree within their
 644 combined error bars, and mostly even within single error bars. The difference between the
 645 members of a pair is much smaller than the distance to any neighbouring value with higher or
 646 lower ordering number in Table 2a. From this it is concluded that the different models find
 647 the same oscillations. The periods of them are obviously quite robust. This and the fact that
 648 **most** boundary conditions have been kept constant makes us believe that these oscillations are
 649 self-excited (intrinsic) oscillations.

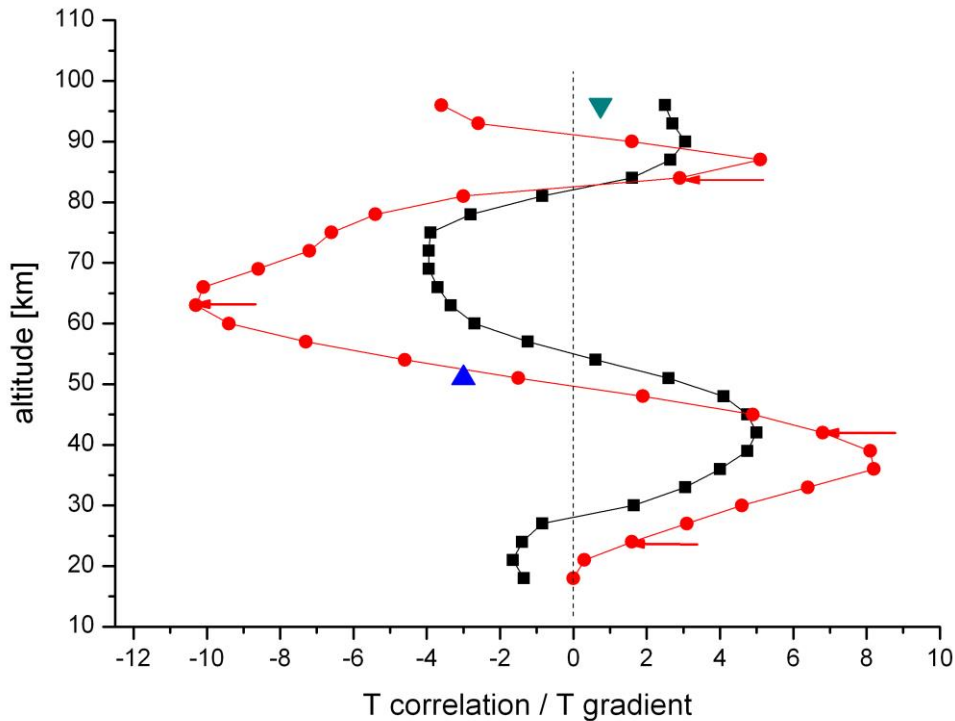
650 A similar agreement is seen for the periods found in the measured Hohenpeißenberg data,
 651 although these have been under the influence of variations of the sun, ocean, and greenhouse
 652 gases. A spectral analysis (auto correlation spectral analysis ASA) of these data is shown in
 653 Fig. 12. It was taken from Schönwiese (1992). The important peak at 3.4 years is not
 654 contained in Table 2, but was found in Offermann et al. (2015). The two peaks near 7.5 yr and
 655 13 yr are close to the values 7.76 ± 0.29 yr and 13.4 ± 0.68 yr in Table 2a.

656 A 335 year long data set of Central England Temperatures (CET) is the longest measured
 657 temperature series available (Plaut et al., 1995). A singular spectrum analysis was applied by
 658 these authors for interannual and interdecadal periods. Periods of 25.0 yr, 14.2 yr, 7.7 yr, and
 659 5.2 yr were identified. All of these values nearly agree with numbers given for HAMMONIA,
 660 WACCM, and/or ECHAM6 in Table 2a (within the error bars given in the Table).

661 Meyer and Kantz (2019) recently studied the data from a large number of European stations
 662 by the method of detrended fluctuation analysis. They identified a period of 7.6 ± 1.8 yr, which
 663 again is in agreement with the HAMMONIA results given in Table 2a (and also agrees with
 664 Fig. 12, and with Plaut et al., 1995).

665 Also the GLOTI data in Table 2a are in agreement with some of the other periods, even
 666 though they are global averages. The results altogether suggest that the periods discussed are
 667 basic (intrinsic) properties of the atmosphere. It will be shown below that they are not limited
 668 to atmospheric temperatures alone, but are, for instance, also seen in Methane mixing ratios.
 669

670
671
672



673
674
675

676 Fig. 13 Comparison of HAMMONIA vertical correlations from Fig. 3 (black squares) with
677 vertical temperature gradients (red dots). Data are from annual mean temperatures.
678 Correlation coefficients are multiplied by 5. Temperature gradients are approximated by the
679 differences of consecutive temperatures (K per 3 km). Two gradients are given for monthly
680 mean temperature curves in addition: blue triangle for January, green inverted triangle for
681 July. Red arrows show the altitudes of the maxima of the accumulated amplitudes in Fig. 11a.

682
683

684 3.4 Oscillation amplitudes

685

686 In an attempt to learn more about the nature of the self-excited oscillations we analyze their
687 oscillation amplitudes. The determination of absolute amplitudes of self-excited oscillations is
688 difficult and beyond the scope of the present paper. Nevertheless, interesting results can be
689 obtained from their relative values. One of these results is related to the vertical gradients of
690 the atmospheric temperature profiles.

691 The HAMMONIA model simulates the atmospheric structure as a whole. The annual mean
692 vertical profile of HAMMONIA temperatures can be derived and is seen to vary between a
693 minimum at the tropopause, a maximum at the stratopause, and another minimum near the
694 mesopause (not shown here). In consequence the vertical temperature gradients change from
695 positive to negative, and to positive again. This is shown in Fig. 13 (red dots) between 18 km
696 and 96 km. The temperature gradients are approximated by the temperature differences of
697 consecutive levels.

698 Also shown in Fig. 13 is the correlation profile of HAMMONIA from Fig. 3 (black squares
699 here). The two curves are surprisingly similar. The similarity suggests some connection of the
700 oscillation structure and the mean thermal structure of the middle atmosphere. This is shown
701 more clearly by the accumulated amplitudes of the self-excited oscillations in Fig. 11a. The
702 maxima of these occur at altitudes near to the extrema of the temperature gradients as is
703 shown by the red arrows in Fig. 13. The mechanism connecting the oscillations and the
704 thermal structure appears to be active throughout the whole altitude range shown (except the
705 lowest altitudes).

706 A possible mechanism might be a vertical displacement of air parcels. If an air column is
707 displaced vertically by some distance D (“displacement height”) a seeming change in mixing
708 ratio is observed at a given altitude. This is a relative change, only, not a photochemical one.
709 It can be estimated by the product $\{D \text{ times mixing ratio gradient}\}$. If the vertical movement
710 is an oscillation, the trace gas variation is an oscillation as well, assuming that D is a constant.
711 Such transports may be best studied by means of a trace gas like CH_4 .

712 HAMMONIA methane mixing ratios have therefore been investigated for oscillation
713 periods in the same way as described above for the temperatures. Results are briefly
714 summarized here.

715 Ten periods have been found, indeed, between 3.56 and 16.75 years by harmonic analyses
716 and are shown in Tab. 3. These periods are very similar to those obtained for the temperatures
717 in Table 2a and 3. The agreement is within the single error bars. Hence it is concluded that the
718 same self-excited oscillations are seen in HAMMONIA temperatures and CH_4 mixing ratios.

719 The CH_4 oscillations support the idea that a displacement mechanism is active. The
720 corresponding displacement heights D were estimated from the CH_4 amplitudes and the
721 vertical gradients of the mean HAMMONIA CH_4 mixing ratios.

722 The values D obtained from the different oscillation periods are about the same, though they
723 show some scatter. This makes us presume that the displacement mechanism may be the same
724 for all oscillations. However, D appears to follow a trend in the vertical direction. The
725 displacements are below 100 m in the lower stratosphere and slowly increase with height to
726 above 200 m.

727 Thus the important result is obtained that the self-excited oscillations are related to a vertical
728 displacement mechanism that is altitude dependent, but appears to be the same for all
729 periods. A more detailed analysis is beyond the scope of this paper.

730
731

732 3.5 Seasonal aspects

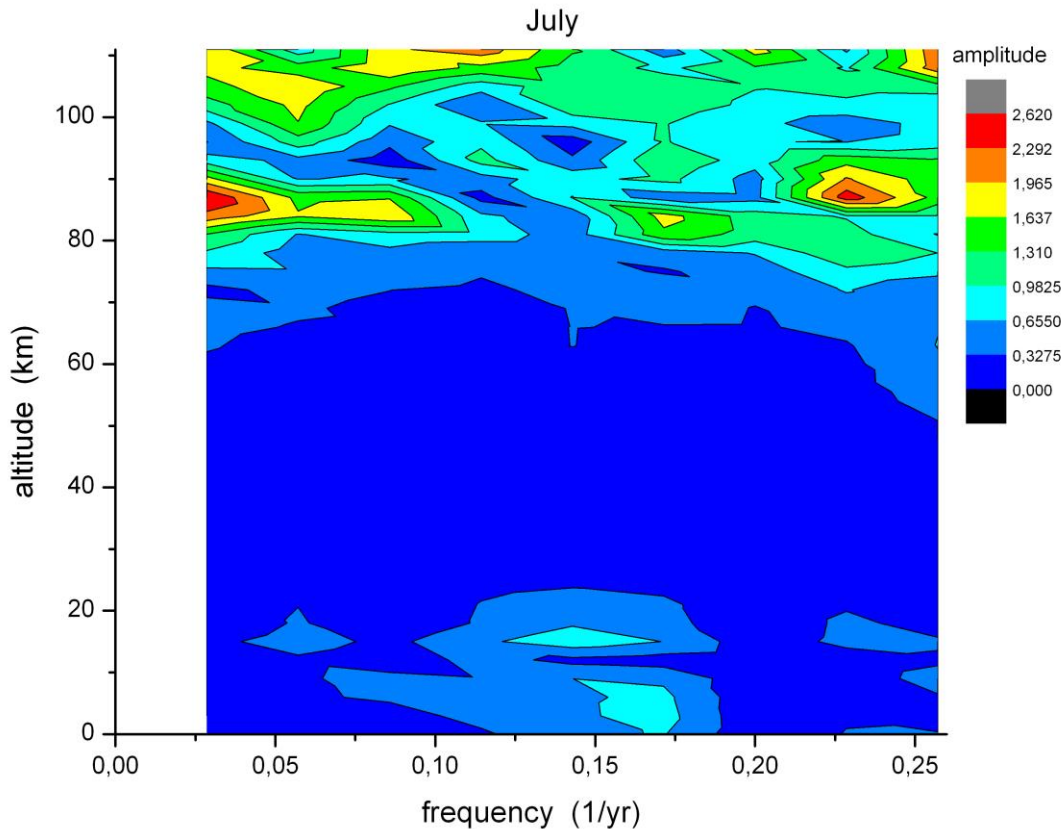
733

734 Our analysis has so far been restricted to annual mean values. Large temperature variations
735 on much shorter time scales are also known to occur in the atmosphere, including vertical
736 correlations (e.g. seasonal variations). This suggests the question whether these might be
737 somehow related to the self-excited, long period oscillations. Our spectral analysis is therefore
738 repeated using monthly mean temperatures of HAMMONIA.

739 Results are shown in Fig. 14 and 15, which give the amplitude distribution vs period and
740 altitude of FFT analyses for the months of July and January. These two months are typical of
741 summer (May-August), and winter (November-March), respectively. In July oscillation
742 amplitudes are seen essentially at altitudes above about 80 km, and some below about 20 km.
743 In the regime in between, oscillations are obviously very small or not excited. The opposite
744 behaviour is seen in January: oscillation amplitudes are now observed in the middle altitude
745 regime where they had been absent in July. This is to be compared to Fig. 6 and 11 that give
746 the annual mean picture. In Fig. 11 the structures (two peaks) above 80 km appear to
747 represent the summer months (Fig. 14). The structures between 80 km and 30 km, on the
748 other hand, apparently are representative of the winter months (Fig. 15).

749 The monthly oscillations appear to be related to the wind field of the HAMMONIA model.
 750 Figure 16 shows the monthly zonal winds of HAMMONIA from the ground up to 111 km
 751 (50°N). Comparison with Fig. 14 and 15 shows that oscillation amplitudes are obviously not
 752 observed in an easterly wind regime. Hence, the long period self-excited oscillations and their
 753 phase changes are apparently related to the dynamical structure of the middle atmosphere. A
 754 change from high to low oscillation activity in the vertical direction appears to be related to a
 755 wind reversal.

756 This correspondence does not, however, exist in all details. In the regimes of oscillation
 757 activity there are substructures. For instance in the middle of the July regime of amplitudes
 758 above 80 km there is a “valley” of low values at about 95 km. A similar valley is seen in the



759 Fig. 14 Self-excited temperature oscillations in the month of July in HAMMONIA.
 760 Amplitudes are shown in dependence of altitude and frequency (periods 3.9-34 yr). Colour
 761 code of amplitudes is in arbitrary units.
 762

763
 764
 765 January data around 55 km. Near these altitudes there are phase changes of about 180° (see
 766 the blue arrows in Fig. 11a). Contrary to our expectation sketched above, these are altitudes of
 767 large westerly zonal wind speeds without much vertical change (see Fig.16). However, the
 768 two “valleys” are relatively close to altitudes where the vertical temperature gradients are
 769 small (see Fig. 13). As the gradients from the annual mean temperatures used for the curves in
 770 Fig. 13 may differ somewhat from the corresponding monthly values two monthly gradients
 771 have been added in Fig. 13 for January (at 51 km) and at 96 km (for July). They are small,
 772 indeed, and could explain low oscillation amplitudes by the above discussed vertical
 773 displacement mechanism.

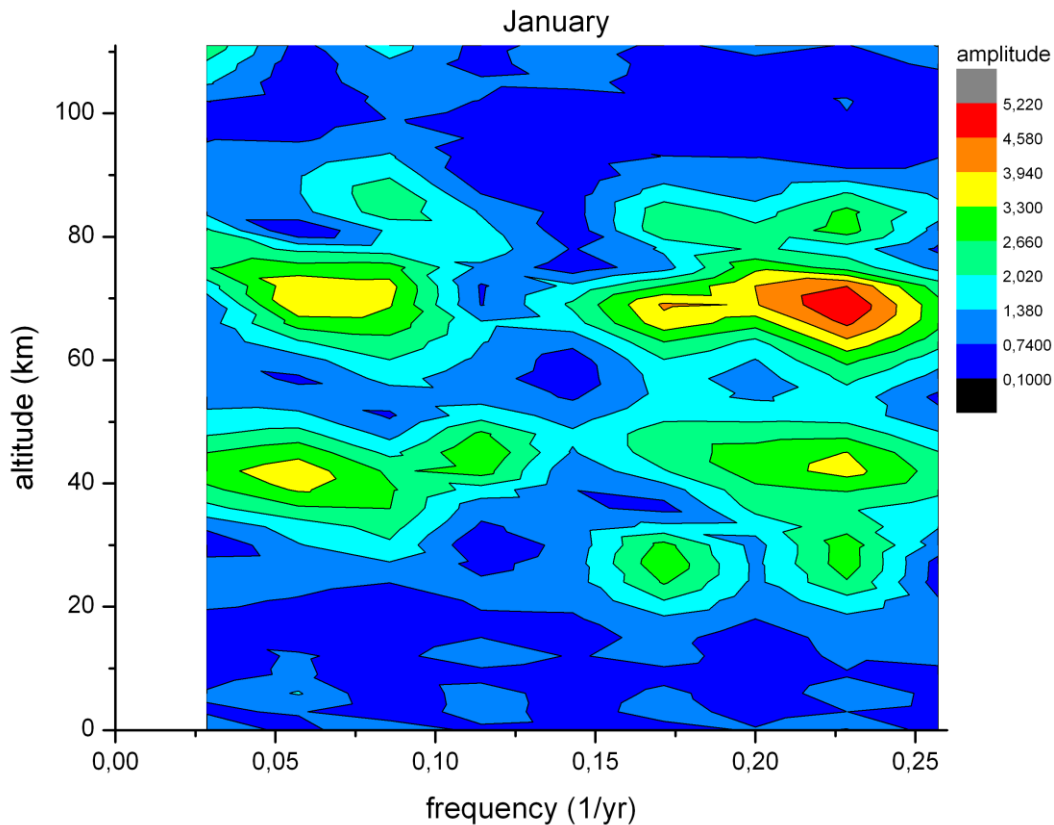
774
 775
 776
 777

778
779
780
781
782
783
784
785
786
787
788
789
790
791
792
793
794
795
796
797

3.6 Oscillation persistence

If our concept of self-excitation of oscillations is correct we might expect that such oscillations might also dissipate after a while, i.e. we should expect some intermittence in our oscillation amplitudes. To check on this we have subdivided the 400 years data record of ECHAM6 in four smaller time intervals (blocks) of 100 years each. In each block we performed harmonic analyses for periods of 24 yr (frequency 0.042/yr) and 37 yr (frequency 0.027/yr), respectively, at the altitudes of 42 km (1.9 hPa) and 63 km (0.11 hPa), respectively. These are altitudes and periods with strong signals as seen in Fig. 7. Results for the two altitudes and two periods are given in Fig. 17.

The results show two groups of amplitudes: one is around 0.15 K, the other is very small and compatible with zero. The two groups are significantly different as is seen from the error bars. This result is compatible with the picture of oscillations being excited and not-excited (dissipated) at different times. The non-excitation (dissipation) for the 24 yr oscillation (black squares) occurs in the first block (century), that for the 37 yr oscillation (red dots) in the second block. The 24 yr profile at 63 km altitude is similar as that at 24 km. Likewise, the 37 yr profile at 24 km is similar to that at 63 km. Hence it appears that the whole atmosphere (or a large part of it) is excited (or dissipated) simultaneously. (The two profiles in Fig. 17 appear to be somehow anticorrelated for some reason that is unknown as yet.)



798
799
800
801
802
803
804
805
806

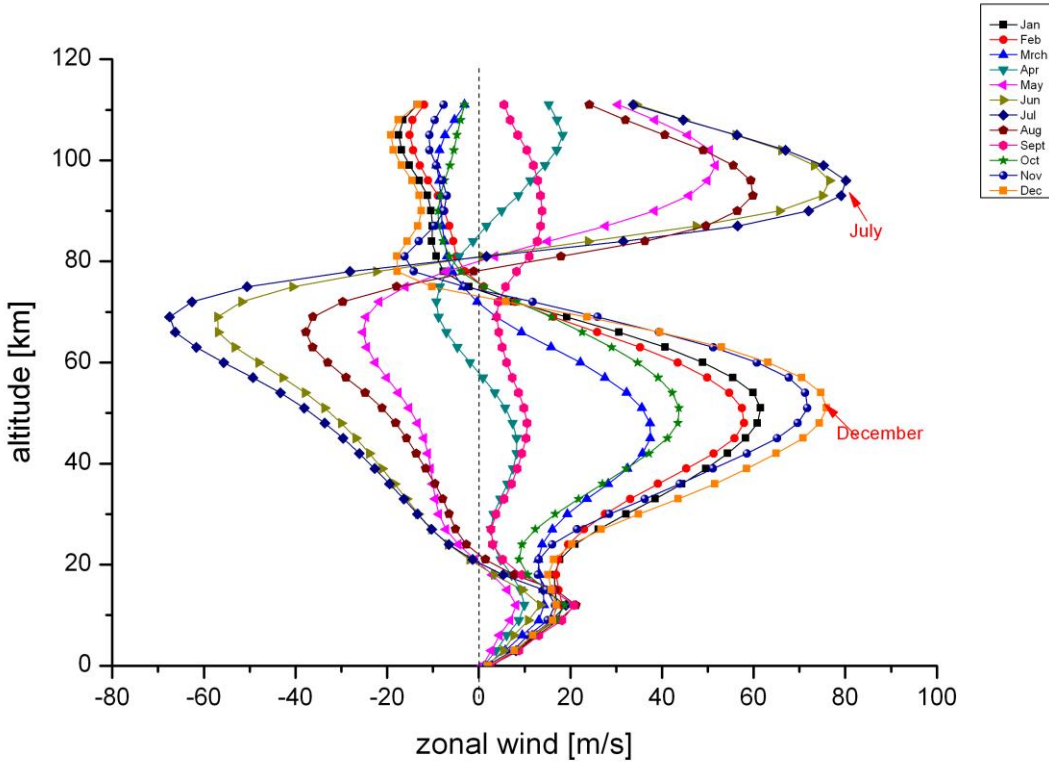
Fig. 15 Self-excited temperature oscillations as in Fig. 14, but for the month of January

For the analysis of shorter periods the 400 year data set of ECHAM6 may be subdivided in a larger number of time intervals. Figure 18 shows the results for periods of 5.4 yr and 16 yr, respectively, for various altitudes. An FFT analysis was performed in 12 equal time intervals (blocks of 32 yr length) in the altitude regime 0.01 – 1000 hPa and the period regime 4 – 40 yr. The corresponding 12 maps look similar as Fig. 15, i.e. there are pronounced amplitude

807 hot spots at various altitudes and periods. (Of course, the values near the 40 yr boundary are
 808 not really meaningful.) In subsequent blocks these hot spots may shift somewhat in altitude
 809 and/or period, and hence the profiles taken at a fixed period and altitude as those of Fig. 18
 810 show some scatter. Nevertheless, there is strong indication of the occurrence of coordinated
 811 high maxima and deep minima of amplitudes in Blocks 3/ 4 and Blocks 10/11, respectively.
 812 These maxima are interpreted as strong oscillation excitation, whereas the minima are
 813 believed to show (at least in part) the dissipation of the oscillations.

814 It should be mentioned that in the FFT analysis the 5.4 yr period is an overtone of the 16 yr
 815 period. Hence the two period data in Fig.18 may be somehow related.

816
817
818
819



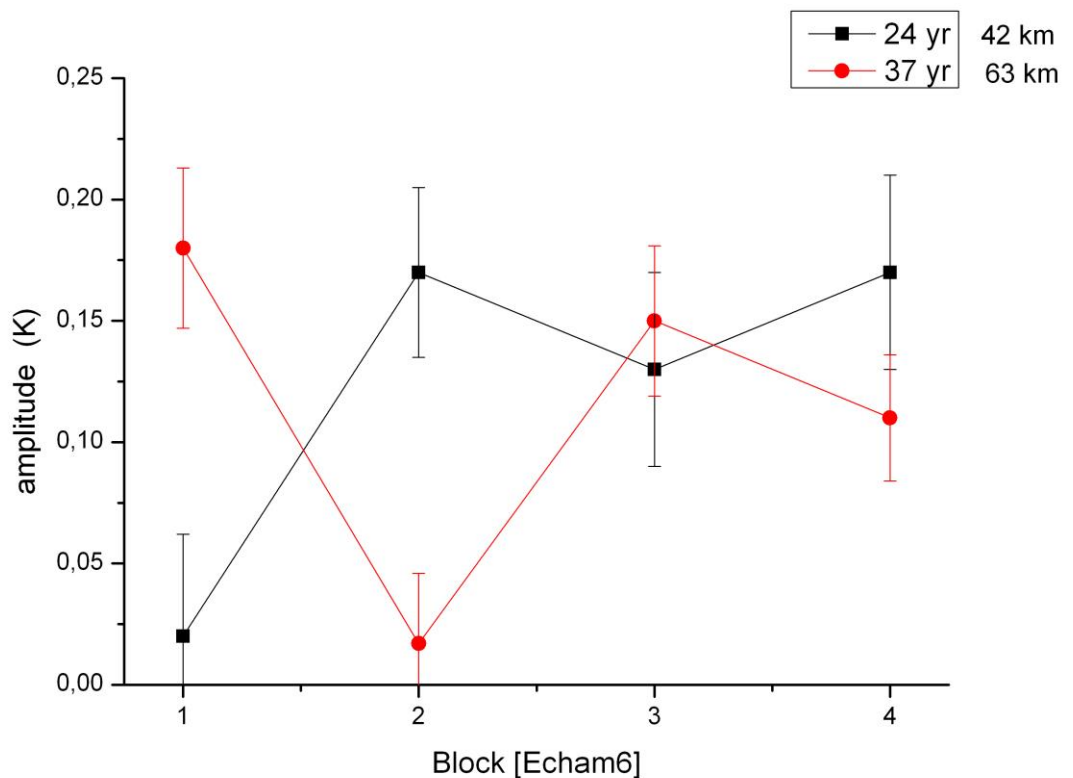
820
821 Fig. 16 Vertical distribution of zonal wind speed in the HAMMONIA model.
822

823
824
825 4 Discussion

826
827 4.1 The nature and origin of the self-excited oscillations are as yet unknown. We therefore
 828 collect here as many of their properties as possible. They do exist in computer models even if
 829 the model boundaries for the influences of the sun, the ocean, the green house gases, etc. are
 830 kept constant. Therefore they are believed to be self-generated oscillations. Further properties
 831 are as follows: **Many of the periods appear to be robust, i.e. they are found with similar values**
 832 in different models. The periods cover a wide range from 2 to above 200 years (at least). The
 833 different oscillations have similar vertical profiles (up to 110 km) of amplitudes and phases.
 834 This may indicate three-dimensional atmospheric oscillation modes. To clarify this, latitudinal
 835 and longitudinal studies of the oscillations are needed in a future analysis.

836
837
838
839
840
841
842
843
844
845
846
847

4.2 The accumulated oscillation amplitudes show a layer structure with alternating maxima and minima and correlations / anticorrelations in the vertical direction. These appear to be influenced by the seasonal variations of temperature and zonal wind in the stratosphere, mesosphere, and lower thermosphere. Table 4 summarizes the results shown in Section 3.5. Maxima of oscillation amplitudes appear to be associated with westerly (eastward) winds together with large temperature gradients (positive or negative). Amplitude minima are associated with either easterly (westward) winds or with near zero temperature gradients. The latter feature is compatible with a possible vertical displacement mechanism. Such displacements can be seen, indeed, in the CH₄ data of the HAMMONIA model. The mechanism summarized in Table 4 appears to be a



848
849
850
851
852
853
854
855
856
857
858
859
860
861
862
863
864

Fig. 17 Amplitudes of 24 yr and 37 yr oscillations in four subsequent equal time intervals (Blocks) of the 400 year data set of ECHAM6.

basic feature of the atmosphere that influences many different parameters as temperature, mixing ratios, etc. Vertical displacements of measured temperature profiles have been discussed for instance by Kalicinsky et al. (2018).

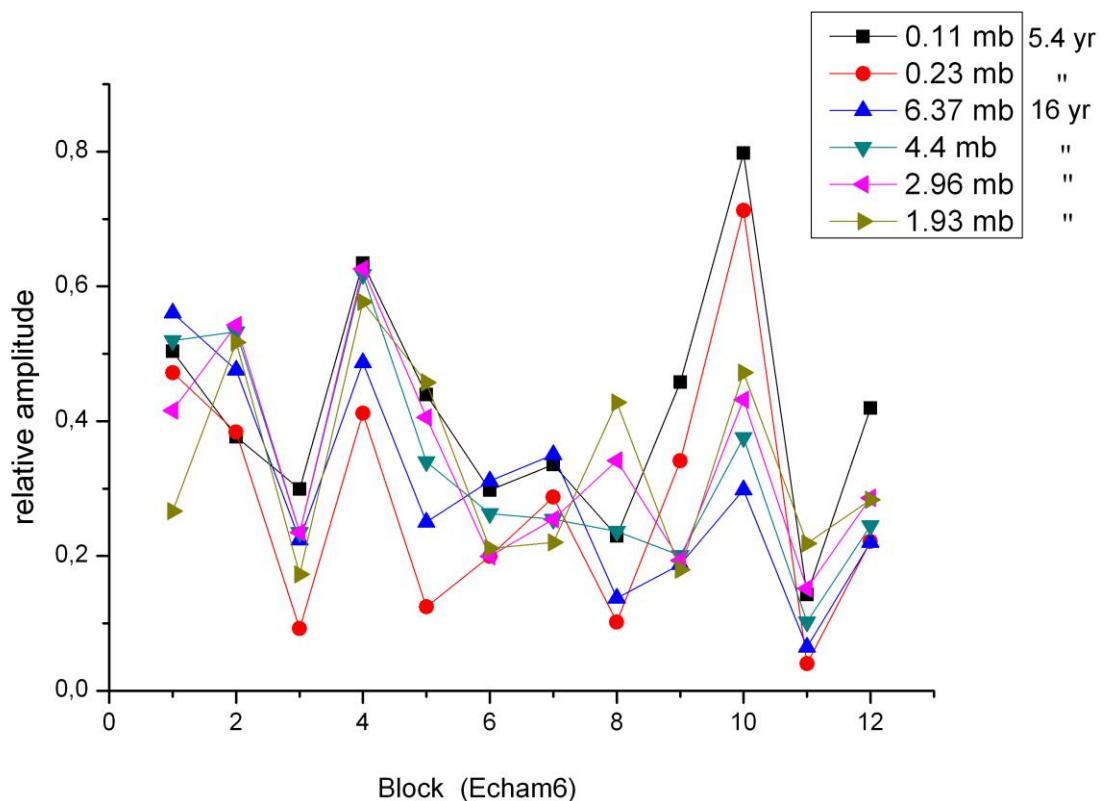
4.3 The amplitudes found for the self-excited oscillations are relatively small (Fig. 1). The question therefore arises whether these oscillations might be spurious peaks, i.e. some sort of noise. We tend to deny the question for the following reasons:

- (a) An accidental agreement of periods as close together as those shown in Table 2a for different model computations appears very unlikely. This also applies to the Hohenpeißenberg data in Table 2a, and several of these periods are even found in the GLOTI data.

865 If the period values were accidental they should be evenly distributed over the
 866 period-space. To study this the range of ECHAM6 periods is
 867 considered. Table 2a shows that the error bars (standard deviations) of ECHAM6
 868 cover approximately half of this range. If the periods of this and some other data set occur at
 869 random, half of them should coincide with the ECHAM6 periods within the
 870 ECHAM6 error bars, and half of them should not. This is checked by means of the
 871 WACCM model data, the Hohenpeissenberg measured data, and three further
 872 measurements sets that reach back to 1783 (Innsbruck, 47.3°N;11.4°E; Vienna,
 873 48.3°N;16.4°E; Stockholm, 59.4°N;18.1°E). The result is that about two thirds of the
 874 periods coincide with ECHAM6 periods within the ECHAM6 error bars. This is far
 875 from an even distribution.

876 It is important to note that the data sets used here are quite different in nature: They are
 877 either model simulations with fixed or partially fixed boundaries, or they are real atmospheric
 878 measurements at different locations.

879
 880



881
 882
 883 Fig. 18 FFT amplitudes of 5.4 yr and 16 yr oscillations in 12 equal time intervals (32 yr
 884 blocks) of the ECHAM6 400 year data set.

885
 886
 887 A further argument against noise is the distribution of the data in Fig. 9 and 10. If our
 888 oscillations were noise, the peaks in these Figures should be evenly distributed with respect to
 889 the period scale. However, the distribution is highly uneven, with high peaks and large gaps,
 890 which is very unlikely to result from noise.

891
 892 (b) The periods given in Table 2a were all calculated by means of harmonic analyses
 893 (Levenberg-Marquardt algorithm). This was done to support the reliability of the comparison

894 of the three models and four measured data sets. There could be, however, the risk of a
895 “common mode failure”. The harmonic analysis results are therefore checked, and are
896 confirmed by the Lomb-Scargle and autocorrelative spectral (ASA) analyses shown in Fig. 8
897 and 12, and by the above cited results of Plaut et al. (1995) and Meyer and Kantz (2019).
898 There is, however, not a one-to-one correspondence of these numbers and those of Table 2a.
899 In general the number of oscillations found by the harmonic analysis is larger. Hence several
900 of the Table 2a periods might be considered questionable. It is also not certain that Table 2a is
901 exhaustive. Nevertheless, the large number of close coincidences is surprising.

902

903 (c) The layered structure of the occurrence of the oscillations (e.g. Fig. 11a) and the
904 corresponding anti-correlations appear impossible to reconcile with a noise field. These
905 correlations extend over about 20 km (or more) in the vertical which is about three scale
906 heights. Turbulent correlation would, however, be expected over one transport length, i.e. one
907 scale height, only.

908

909 (d) The apparent relation of the oscillations to the zonal wind field and the vertical
910 temperature structure (Table 4) would be very difficult to be explained by noise.

911

912 (e) The close agreement (within single error bars) of the oscillation periods in
913 temperatures and in CH₄ mixing ratios would also be very difficult to be explained by
914 noise.

915

916 In summary it appears that many of the oscillations are intrinsic properties of the
917 atmosphere that are also found in sophisticated simulations of the atmosphere.

918

919

920 4.4 The self-excited oscillations are studied here mainly for atmospheric temperatures.
921 They show up, however, in a similar way in other parameters as winds, pressure, trace gas
922 densities, NAO, etc. (Offermann et al., 2015). Some of the periods in Table 2a appear to be
923 similar to the internal decadal variability of the atmosphere/ocean system (e.g., Meehl et al.,
924 2013; 2016; Fyfe et al. 2016). One example is the Atlantic Multidecadal Oscillation (AMO)
925 as discussed by Deser et al. (2010) with time scales of 65-80 yr, and with its “precise nature
926 ...still being refined”. Variability on centennial time scales and its internal forcing was
927 recently discussed by Dijkstra and von der Heydt (2017). It needs to be emphasized that the
928 oscillations discussed in the present paper are not caused by the ocean as they occur even if
929 the ocean boundaries are kept constant.

930

931 4.5 The self-excited oscillations obviously are somehow related to the “internal
932 variability” discussed in the atmosphere/ocean literature at 40 – 80 years time scales (“climate
933 noise”, see e.g. Deser et al., 2012, Gray et al., 2004, and other references in Section 1). The
934 particular result of the present analysis is its extent from the ground up to 110 km, showing
935 systematic structures in all of this altitude regime. These vertical structures lead us to hope
936 that the nature of the oscillations and hence of (part of) the “internal variability” can be
937 revealed in the future.

938

939 4.6 It appears that the time persistency of the self-excited oscillations is limited. Longer
940 data sets are needed to study this further.

941

942 4.7 The internal variability in the atmosphere/ocean system “...makes an appreciable
943 contribution to the total... uncertainty in the future (simulated) climate response...” (Deser et
944 al., 2012). Similarly our self-excited oscillations might interfere with long term (trend)

945 analyses of various atmospheric parameters. This includes slow temperature increases as part
946 of the long term climate change, and needs to be studied further.

947
948
949

950 5 Summary and Conclusions

951

952 The structures analyzed in this paper are believed to be oscillations that are self-generated
953 in the atmosphere. The oscillations occur in a similar way in different atmospheric climate
954 models, and even when the boundary conditions of sun, ocean, and greenhouse gases are kept
955 constant. They also occur in long-term temperature measurements series. They are
956 characterized by a large range of period values from below 5 to beyond 200 years. Periods of
957 self-excited oscillations are known to be robust. This is in line with the fact that we find very
958 nearly the same periods in different climate model calculations as well as in long observation
959 series.

960 As we do not yet understand the nature of the oscillation structures we try to assemble as
961 many of their properties as possible. The oscillations show typical and consistent structures in
962 their vertical profiles. Temperature amplitudes show a layered behaviour in the vertical
963 direction with alternating maxima and minima. Phase profiles are also layered with 180°
964 phase jumps near the altitudes of the amplitude minima (anticorrelations). There are also
965 indications of vertical transports suggesting a displacement mechanism in the atmosphere. As
966 an important result we find that for all oscillation periods the altitude profiles of amplitudes
967 and phases as well as the displacement heights are nearly the same. This leads us to suspect an
968 atmospheric oscillation mode.

969 These signatures are found to be related to the thermal and dynamical structure of the
970 middle atmosphere. They are seen to be an essential part of atmospheric dynamics. All results
971 presently available are local, i.e. they refer to the latitude and longitude of Central Europe. In
972 a future step horizontal investigations need to be performed to check on a possible modal
973 structure.

974 Most of the present results are for temperatures at various altitudes (up to 110 km). Other
975 atmospheric parameters indicate a similar behaviour and need to be analyzed in detail in the
976 future. Also, the potential of the long period oscillations to interfere with trend analyses needs
977 to be investigated.

978
979
980
981
982
983
984
985
986
987
988
989
990
991
992
993
994
995

996
997
998
999
1000
1001
1002
1003
1004
1005
1006
1007
1008
1009
1010
1011
1012
1013
1014
1015
1016
1017
1018
1019
1020
1021
1022
1023
1024
1025
1026
1027
1028
1029
1030
1031
1032
1033
1034
1035
1036
1037
1038
1039
1040
1041
1042
1043
1044
1045
1046

Author contribution

DO performed data analysis and prepared the manuscript and figures with contributions from all co-authors.

JW managed data collection and performed FFT spectral analyses.

ChK performed Lomb-Scargle spectral and statistical analyses

RK provided interpretation and editing of the manuscript, figures, and references.

Competing Interests

The authors declare that they have no conflict of interest.

1047
1048
1049 Acknowledgements

1050
1051
1052
1053 Global Land Ocean Temperature Index (GLOTI) data were downloaded from
1054 http://data.giss.nasa.gov/gistemp/tabledata_v3/GLB.Ts+dSST.txt and are gratefully
1055 acknowledged..

1056
1057 We thank Katja Matthes (GEOMAR, Kiel, Germany) for making available the WACCM4
1058 data, and for helpful discussions. Model integrations of the CESM-WACCM Model have
1059 been performed at the Deutsches Klimarechenzentrum (DKRZ) Hamburg, Germany. The help
1060 of Sebastian Wahl in preparing the CESM-WACCM data is greatly appreciated.

1061
1062 HAMMONIA and ECHAM6 simulations were performed at and supported by the German
1063 Climate Computing Centre (DKRZ). Many and helpful discussions with Hauke Schmidt (MPI
1064 Meteorology, Hamburg, Germany) are gratefully acknowledged.

1065
1066 We are grateful to Wolfgang Steinbrecht (DWD, Hohenpeißenberg Observatory, Germany)
1067 for the Hohenpeißenberg data and many helpful discussions.

1068
1069 Part of this work was funded within the project MALODY of the ROMIC program of the
1070
1071 German Ministry of Education and Research under Grant No. 01LG1207A

1072
1073
1074 **We thank three referees for their detailed and thoughtful comments.**

1075
1076
1077
1078
1079
1080
1081
1082

1083
1084 References.
1085
1086 Biondi, F., Gershunov, A., and Cayan, D.R.: North Pacific Decadal Climate Variability since
1087 1661, *J. Climate* 14, 5-10, 2001.
1088
1089 Dai, A, Fyfe, J.C., Xie, Sh.-P., and Dai, X,: 2015.: Decadal modulation of global surface
1090 temperature by internal climate variability, *Nature Climate Change*,
1091 doi:10.1036/NCLIMATE2605 , 2015.
1092
1093 Deser, C. Alexander, M.A., Xie,S.P., Phillips, A.S.: Sea surface temperature variability:
1094 patterns and mechanisms, *Ann. Rev. Mar. Sci.*,2, 115-143, 2010.
1095
1096 Deser, C., Phillips, A., Bourdette, V., and Teng, H.: Uncertainty in climate change
1097 projections: the role of internal variability, *Clim. Dyn.*, 38, 527-546, 2012.
1098
1099 Deser, C., Phillips, A.S., Alexander, M.A., and Smoliak, B.V.: Projecting North American
1100 climate over the next 50 years: Uncertainty due to internal variability, *J.Climate*, 27, 2271-
1101 2296, 2014.
1102
1103 Dijkstra, H.A., te Raa, L., Schmeits, M., and Gerrits, J.: On the physics of the Atlantic
1104 Multidecadal Oscillation, *Ocean Dynamics*, DOI: 10/1007/s10236-005-0043-0, 2005.
1105
1106 Dijkstra, H.A., and von der Heydt, A.S.: Basic mechanisms of centennial climate variability,
1107 *Pages Magazine*, Vol.25, No.3, 2017.
1108
1109 Flato, G., et al. : Evaluation of Climate Models, in: *Climate Change 2013: The Physical*
1110 *Science Basis*, Contribution of Working Group I to the Fifth Assessment Report of the
1111 Intergovernmental Panel on Climate Change, (eds..Stocker, T.E., et al.) Ch.9, IPCC,
1112 Cambridge Univ.Press, UK and New York, NY, USA, 2013.
1113
1114 Fyfe, J. C., Meehl, G.A., England, M.H., Mann, M.E., Santer, B.D., Flato, G.M., Hawkins,
1115 E., Gillett, N.P., Xie, Sh.P., Kosaka, Y., and Swart, N.C.: Making sense of the early-2000s
1116 warming slowdown, *Nature Climate Change*, 6, 224-228, 2016.
1117
1118 Giorgetta, M. et al.: Climate and carbon cycle changes from 1850 to 2100 in MPI-ESM
1119 simulations for the coupled model intercomparison project phase 5, *J. Adv. Model. Earth*
1120 *Syst*, 5, 572-597, doi:10.1002/jame.20038, 2013.
1121
1122 Gray, ST.T., Graumlich, L.J., Betancourt, J.L., and Pederson, G.T.: A tree-ring based
1123 reconstruction of the Atlantic Multidecadal Oscillation since 1567 A.D.. *Geophys.Res.Lett.*,
1124 31, L 12205, doi:10.1029/2004GL019932 2004.
1125
1126 Hansen, F., Matthes, K., Petrick, C., and Wang, W.: 2014. The influence of natural and
1127 anthropogenic factors on major stratospheric sudden warmings. *J.Geophys.Res. Atmos.*, 119,
1128 8117-8136, 2014.
1129
1130 Hansen, J., Ruedy, Sato, M., and Lo, K.: Global Surface Temperature Change, *Rev.Geophys.*,
1131 48, RG 4004, 2010.
1132 .

1133 Kalicinsky, Ch., Knieling, P., Koppmann, R., Offermann, D., Steinbrecht, W., and Wintel,
1134 J.: 2016. Long term dynamics of OH* temperatures over Middle Europe: Trends and solar
1135 correlations, *Atmos. Chem. Phys.*, 16, 15033 – 15047, 2016.

1136
1137 Kalicinsky, CH., Peters, D.H.W., Entzian, G., Knieling, P., and Matthias, V.: Observational
1138 evidence for a quasi-bidecadal oscillation in the summer mesopause region over Western
1139 Europe, *J. Atmos. Sol.-Terr. Phys.*, 178, 7 – 16., doi.org/10.1016/j.jastp.2018.05.008, 2018.

1140
1141 Karnauskas, K. B., Smerdon, J.E., Seager, R., and Gonzalez-Rouco, J.F. : A pacific centennial
1142 oscillation predicted by coupled GCMs, *JCLI* September 2012, doi:10.1175/JCLI-D-11-
1143 00421.1, 2012.

1144
1145 Kinnison, D., Brasseur, G.P., Walters, S., et al. : Sensitivity of chemical tracers to
1146 meteorological parameters in the MOZART-3 chemical transport model. *J.Geophys.Res.*,
1147 112, D20302, doi :10.1029/2006JD007879, 2007.

1148
1149 Latif, M., Martin, T., and Park, W.: Southern ocean sector centennial climate variability and
1150 recent decadal trends, *J. Climate*, 26, 7767-7782, 2013.

1151
1152 Lean,J., Rottman, G., Harder, J., and G.Knopp, G.: SOURCE contributions to new
1153 understanding of global change and solar variability, *Sol.Phys.* 230, 27-53.
1154 doi:10.1007/S11207-005-1527-2, 2005.

1155
1156 Lomb, N.R., Least-squares frequency analysis of unequally spaced data, *Astrophys.Space*
1157 *Sci.*, 39, 447-462, 1976.

1158
1159 Lu, J., Hu, A., and Zeng, Z.: On the possible interaction between internal climate variability
1160 and forced climate change, *Geophys. Res. Lett.*, 41, 2962-2970, 2014.

1161
1162 Mantua, N.J., and Hare, St.R.: ThePacific Decadal Oscillation. *J.Oceanography*, 58, 35,2002.

1163
1164 Matthes, K., Kodera, K., Garcia, R.R., Kuroda, Y., Marsh, D.R., and Labitzke, K.: The
1165 importance of time-varying forcing for QBO modulation of the atmospheric 11 year solar
1166 cycle signal, *J.Geophys.Res.*, 118, 4435-4447, 2013.

1167
1168 Meehl, G.A., Hu, A., Arblaster, J., Fasullo, J., and Trenberth, K.E.: Externally forced and
1169 internally generated decadal climate variability associated with the Interdecadal Pacific
1170 Oscillation, *J.Cimate*, 26, 7298-7310, 2013.

1171
1172 Meehl, G.A., Hu, A., Santer, B.D., and Xie, SH.-P.: Contribution of Interdecadal Pacific
1173 Oscillation to twentieth-century global surface temperature trends. *Nature Climate Change*,
1174 6,1005-1008, doi:10.1038/nclimate3107, 2016.

1175
1176 Meyer, P.G., and Kantz, H.: A simple decomposition of European temperature variability
1177 capturing the variance from days to a decade, *Climate Dynamics*, 53, 6909-6917,
1178 doi.org/10.1007/s00382-019-04965-0, 2019.

1179
1180 Minobe, Sh.: A 50-70 year climatic oscillation over the North Pacific and North America,
1181 *Geophys.Res.Lett.*, 24, 683-686, 1997.

1182

1183 Offermann, D., Goussev, O., Kalicinsky, Ch., Koppmann, R., Matthes, K., Schmidt, H.,
1184 Steinbrecht, W., and J. Wintel, J.: A case study of multi-annual temperature oscillations in
1185 the atmosphere: Middle Europe, *J.Atmos.Sol.-Terr.Phys.*, 135, 1-11, 2015.

1186
1187 Plaut, G., Ghil, M., and Vautard, R.: Interannual and interdecadal variability in 335 years of
1188 Central England Temperatures, *Science*, 268, 710 – 713, 1995.

1189
1190 Paul, A., and M. Schulz, M.: Holocene climate variability on centennial-to-millennial time
1191 scales: 2. Internal and forced oscillations as possible causes. In: Wefer,G., W.Berger, K-E.
1192 Behre, and E. Jansen (eds), 2002, *Climate development and history of the North Atlantic*
1193 *realm*, Springer, Berlin, Heidelberg, 55-73, 2002.

1194
1195 Polyakov,I.V. Berkryaev, R.V., Alekseev,G.V., Bhatt, U.S., Colony, R.L., Johnson, M.A.,
1196 Maskstas, A.P., and Walsh, D.: Variability and trends of air temperature and pressure in the
1197 Maritime Arctic, 1875-2000, *J.Climate*, 16, 2067-2077, 2003.

1198
1199 Roeckner, E., Brokopf, R., Esch, M., Giorgetta, M., Hagemann, S., Kornblueh, L., Manzini,
1200 E., Schlese, U., Schulzweida, U.: Sensitivity of simulated climate to horizontal and vertical
1201 resolution in the ECHAM5 atmosphere model, *J.Clim.*, 19, 3771–3791, 2006.

1202
1203 Scargle, J.D.: Studies in astronomical time series analysis. II. Statistical aspects of spectral
1204 analysis of unevenly spaced data, *Astrophys.J.*, 263, 835-853, 1982.

1205
1206 Schlesinger, M.E. and N. Ramankutty, N.: An oscillation in the gobal climate system of
1207 period 65-70 years, *Nature*, 367, 723-726, 1994.

1208
1209 Schmidt, H., Brasseur, G.P., Charron, M., Manzini, E., Giorgetta, M.A., Diehl,T., Fo-
1210 michev, V.I., Kinnison, D., Marsh, D., Walters, S.: The HAMMONIA chemistry climate
1211 model: Sensitivity of the mesopause region to the 11-year solar cycle and CO2 doubling, *J.*
1212 *Clim*, 19, 3903–3931, <http://dx.doi.org/10.1175/JCLI3829.1>, 2006.

1213
1214 Schmidt, H., Brasseur, G.P., and Giorgetta, M.A.:2010. The solar cycle signal in a general
1215 circulation and chemistry model with internally generated quasi-biennial oscillation. *J.*
1216 *Geophys. Res.* 115, 8, doi :10.1029/2009JD012542, 2010.

1217
1218 Schönwiese, Ch.-D.: *Praktische Statistik für Meteorologen und Geowissenschaftler*,
1219 2.Auflage, Gebrüder Borntraeger, Berlin, Stuttgart, Abb.57, page 185, [www.borntraeger-](http://www.borntraeger-cramer.de/9783443010294)
1220 [cramer.de/9783443010294](http://www.borntraeger-cramer.de/9783443010294), 1992.

1221
1222 Soon, W. W.-H.: Variable solar irradiance as a plausible agent for multidecadal variations in
1223 the Arctic-wide surface air temperature record of the past 130 years, *Geophys.Res.Lett.*, 32,
1224 L16712, doi:10.1029/2005GL023429 2005.

1225
1226 Stevens, B., Giorgetta, M., Esch, M., Mauritsen, T., Crueger, T., Rast, S., Salzmann, M.,
1227 Schmidt, H., Bader, J., Block, K., Brokopf, R., Fast, I., Kinne, S., Kornblueh, L., Lohmann,
1228 U., Pincus, R., Reichler, T., and Roeckner, E.: The atmospheric component of the MPI-M
1229 earth system model: ECHAM6, *J. Adv. Model. Earth Syst.*, 5, 1-27, 2013.

1230
1231 White, W.B., and Liu, Z.: Non-linear alignment of El Nino to the 11-yr solar cycle,
1232 *Geophys.Res.Lett.*, 35, L19607, doi:10.1029/2008GL034831, 2008.

1233

1234 Xu, D., Lu, H., Chu, G., Wu, N., Shen, C., Wang, C., and Mao, L.: 500-year climate cycles
1235 stacking of recent centennial warming documented in an East Asian pollen record,
1236 Scientific Reports , 4, No.3611, doi:10.1038/srep03611, 2014.

1237
1238
1239
1240
1241
1242
1243
1244
1245
1246
1247
1248
1249
1250
1251
1252
1253
1254
1255
1256
1257
1258
1259
1260
1261
1262
1263
1264
1265
1266
1267
1268
1269
1270
1271
1272
1273
1274
1275
1276
1277
1278
1279
1280
1281
1282
1283
1284
1285

1286
1287
1288
1289
1290
1291
1292
1293
1294
1295
1296
1297
1298
1299
1300
1301
1302
1303
1304
1305
1306
1307
1308
1309
1310
1311
1312
1313
1314
1315
1316
1317
1318
1319
1320
1321
1322
1323
1324
1325
1326
1327
1328
1329
1330
1331
1332
1333
1334
1335
1336
1337
1338
1339
1340
1341
1342

Table 1

Properties of the GCM simulations

All data are for Central Europe (50°N, 7°E). For various details see text.

	HAMMONIA	WACCM4	ECHAM6
Horizontal resolution	T31	1.9°x2.5° (lat/long)	T63
Vertical resolution	119 levels 1 km (stratosphere)	66 levels	47 levels
altitude range	0 – 110 km	0 – 108 km	0 – 78 km
length of simulation	34 yr	150 yr	400 yr
time resolution of data used	annual/monthly	annual	annual
boundary conditions			
- sun	fixed	variable (see text)	fixed
- ocean	climatological SST and sea ice	climatological SST and sea ice	climatological SST and sea ice
- greenhouse gases	fixed	fixed (1960 values)	fixed
References	Schmidt et al., 2010	Hansen et al., 2014	Stevens et al., 2013

1343
 1344
 1345
 1346
 1347
 1348
 1349
 1350
 1351
 1352
 1353
 1354
 1355
 1356
 1357
 1358
 1359
 1360
 1361
 1362
 1363
 1364
 1365
 1366
 1367
 1368
 1369
 1370
 1371
 1372
 1373
 1374
 1375
 1376
 1377
 1378
 1379
 1380
 1381
 1382
 1383
 1384
 1385
 1386
 1387
 1388
 1389
 1390
 1391
 1392
 1393
 1394
 1395

Table 2a:

Periods of temperature oscillations from harmonic analyses

Periods are numbered according to increasing values. Periods (in years) are given with their standard deviations. Self-excited periods are from the HAMMONIA, WACCM, and ECHAM6 models, respectively. Additional periods are from Hohenpeißenberg measurements, and from the Global Land Ocean Temperature Index (GLOTI).

HAMMONIA periods are limited to 28.5 yr as the model run covered 34 yr, only.

WACCM periods are given below 147 yr from a model run of 150 yr. ECHAM6 periods are from a 400 yr run.

Short periods (below 20 yr) are not shown for WACCM, ECHAM6, and GLOTI as they are not used in the present paper. Hohenpeißenberg and GLOTI data after 1980 are not included in the analyses because of their steep increase in later years.

Periods given in bold type refer to Tab. 2b.

No	HAMMONIA (119 layers) (years)		WACCM (years)		ECHAM6 (47 layers) (years)		Hohenpeißenberg 1783 – 1980 (years)		GLOTI 1880 - 1980 (years)	
1	5.34	± 0.1					5.48	±0.21		
2	6.56	0.24					6.16	0.20		
3	7.76	0.29					7.83	0.26		
4	9.21	0.53					9.50	0.65		
5	10.8	0.34					10.85	0.38		
6	13.4	0.68					13.6	0.80		
7	17.3	1.05					18.02	1.08		
8	--	--			20.0	±0.35	19.9	± 1		20.2 ± 1.36
9	--	--			20.9	0.15	--	--		
10	22.8	1.27	21.7	± 1.02	22.1	0.23	21.9	0.94		
11	--	--			23.8	0.42				
12	--	--	25.82	0.86	25.3	0.46	25.1	0.62	25.5	2.0
13	28.5	1.63	--	--	27.3	0.41	--	--		
14			31.56	1.42	30.2	0.49	29.8	0.66		
15			--	--	33.3	0.84	--	--		
16			38.1	0.82	36.9	1.17	36.01	1.28	35.4	2.42
17			41.89	0.95	41.4	0.97	--	--		
18			--	--	48.4	1.73	--	--		
19			--	--	--	--	52.06	1.61	53.4	11.4
20			57.64	1.69	58.3	1.77	--	--		
21			66.95	7.31	64.9	2.98	--	--		
22			--	--	77.5	3.94	81.6	4.18		
23			97.27	5.06	95.5	5.86	--	--		
24			147	14.9	129.4	14.5	--	--		
25					206.7	16.3	--	--		
26					--	--	238.2	11.8		

1396
1397
1398
1399
1400
1401
1402
1403
1404
1405
1406
1407
1408
1409
1410
1411
1412
1413
1414
1415
1416
1417
1418
1419
1420
1421
1422
1423
1424
1425
1426
1427
1428
1429
1430
1431
1432
1433
1434
1435
1436
1437
1438
1439
1440
1441
1442
1443
1444
1445
1446
1447
1448
1449
1450
1451
1452
1453
1454
1455
1456

Table 2b Comparative periods (in years)

Period (yr) from HAMMONIA/ECHAM6 (numbers refer to Tab. 2a)	Accuracy/Significance (SSA: Single Spectrum Analysis) (ASA: Auto correlation Spectral Analysis) (DFA: Detrended Fluctuation Analysis)	Source/corresponding period
#1 5.34 ± 0.1	2 σ	- Lomb-Scargle periodogram as in Fig. 8 (not shown here)
	SSA	- Plaut et al. (1995) : 5.2 yr
#2 6.56 ± 0.24	1 σ	- Lomb-Scargle periodogram as in Fig.8 (not shown here)
		- see also CH4 analysis (Tab.3): 6.43 + 0.26 yr
#3 7.76 ± 0.29	SSA	- Plaut et al. (1995) : 7.7 yr
	ASA (80 %)	- Schönwiese (1992) : 7.5 yr
	DFA	- Meyer and Kantz (2019) : 7.6 ±1.8 yr
#6 13.4 ± 0.68	SSA	- Plaut et al. (1995) : 14.2 yr
	ASA (95%)	- Schönwiese (1992): 13 yr
	2 σ	- Lomb-Scargle periodogram as in Fig.8 (not shown here)
		- see also CH4 analysis (Tab.3) : 13.73 ± 0.93 yr
#7 17.3 ± 1.05	2 σ	- Lomb-Scargle periodogram as in Fig. 8 (not shown here)
#10 21.1 ± 0.23	1 σ	- Lomb-Scargle periodogram : 22.3 yr , see Fig.8
#12 25.3 ± 0.46	SSA	- Plaut et al. (1995) : 25.0 yr
#14 30.2 ± 0.49	2 σ	- Lomb-Scargle periodogram : 30.4 yr see Fig.8
#17 41.4 ± 0.97	2 σ	- Lomb-Scargle periodogram : 40.7 yr see Fig.8
#18 48.4 ± 1.73	2 σ	- Lomb-Scargle periodogram : 48.1 yr see Fig.8
#20 58.3 ± 1.77	1 σ	- Lomb-Scargle periodogram: 58.9 yr see Fig. 8

1457
 1458
 1459
 1460
 1461
 1462
 1463
 1464
 1465
 1466
 1467
 1468
 1469
 1470
 1471
 1472
 1473
 1474
 1475
 1476
 1477
 1478
 1479
 1480
 1481
 1482
 1483
 1484
 1485
 1486
 1487
 1488
 1489
 1490
 1491
 1492
 1493
 1494
 1495
 1496
 1497
 1498
 1499
 1500
 1501
 1502
 1503
 1504
 1505
 1506
 1507
 1508

Table 3

Period comparison of two different HAMMONIA runs: temperature and CH4

Periods (in years) are given together with their standard deviations.
 HAMMONIA run Hhi-max (temperature and CH4 mixing ratios) uses 119 altitude layers and covers 34 years;
 run Hlo-max uses 67 layers and covers 20 years.

No	Hhi-max (temperature)		Hlo-max (temperature)		CH4	
1	2.06	± 0.02	2.07	± 0.04		
2	2.16	0.02	2.15	0.02		
3	2.33	0.04	2.36	0.03		
4	2.51	0.04	2.43	0.02		
5	2.79	0.08	2.78	0.07		
6	3.11	0.08	3.2	0.09		
7	3.52	0.12	3.44	0.15	3.56	± 0.15
8	3.96	0.08	3.9	0.12	4.02	0.17
9	4.48	0.21	4.27	0.21	4.57	0.17
10	5.34	0.1	5.48	0.29	5.41	0.29
11	6.56	0.24	6.57	0.29	6.43	0.26
12	7.76	0.29	8.02	0.12	7.9	0.45
13	9.21	0.53	9.16	0.33	9.38	0.47
14	10.8	0.34	11.05	0.46	10.93	0.61
15	13.4	0.68	13.02	0.83	13.73	0.93
16	17.3	1.05	--	--	16.75	0.9
17	22.8	1.27	22.68	1.11		

1509
1510
1511
1512
1513
1514
1515
1516
1517
1518
1519
1520
1521
1522
1523
1524
1525
1526
1527
1528
1529
1530
1531
1532
1533
1534
1535
1536
1537
1538
1539
1540
1541
1542
1543
1544
1545
1546
1547
1548
1549
1550
1551
1552
1553
1554
1555
1556
1557
1558
1559

Table 4

Maxima / minima of accumulated amplitudes of temperature oscillations and associated structures (see Fig. 11a)
(stratosphere, mesosphere, lower thermosphere)

altitude (km)	accumulated amplitudes	zonal wind	temperature gradient
105	max	westerly (summer)	large (positive)
93	min	westerly (summer)	near zero
84	max	westerly (summer)	large (positive)
78	min	easterly (except Sept)	medium (negative)
63	max	westerly (winter)	large (negative)
51	min	westerly (winter)	near zero
42	max	westerly (winter)	large (positive)

1560
1561
1562
1563
1564
1565
1566
1567
1568
1569
1570
1571
1572
1573
1574
1575
1576
1577
1578
1579
1580
1581
1582
1583
1584
1585
1586
1587
1588
1589
1590
1591
1592
1593
1594
1595
1596
1597
1598
1599
1600
1601
1602
1603
1604
1605
1606
1607
1608
1609
1610
1611
1612
1613
1614
1615
1616

Table 5

List of Acronyms

Acronym

Definition

CCM	Chemistry Climate Model
CESM-WACCM	Community Earth System Model – Whole Atmosphere Community Climate Model
ECHAM6	ECMWF/Hamburg
GLOTI	Global Land Ocean Temperature Index
HAMMONIA	HAMBURG Model of the Neutral and Ionized Atmosphere
IPCC	Intergovernmental Panel on Climate Change
LOTI	Land Ocean Temperature Index